Insights into Gastrointestinal Redox Dysregulation in a Rat Model of Alzheimer's Disease and the Assessment of the Protective Potential of D-Galactose

Homolak, Jan; Varvaras, Konstantinos; Sciacca, Vittorio; Babić Perhoč, Ana; Virag, Davor; Knezović, Ana; Osmanović Barilar, Jelena; Šalković-Petrišić, Melita

Article

Insights into Gastrointestinal Redox Dysregulation in a Rat Model of Alzheimer's Disease and the Assessment of the Protective Potential of D-Galactose

Jan Homolak,* Konstantinos Varvaras, Vittorio Sciacca, Ana Babic Perhoc, Davor Virag, Ana Knezovic, Jelena Osmanovic Barilar, and Melita Salkovic-Petrisic

Read Online

ACCESS | Metrics & More | Article Recommendations

ABSTRACT: Recent evidence suggests that the gut plays a vital role in the development and progression of Alzheimer's disease (AD) by triggering systemic inflammation and oxidative stress. The well-established rat model of AD, induced by intracerebroventricular administration of streptozotocin (STZ-icv), provides valuable insights into the GI implications of neurodegeneration. Notably, this model leads to pathophysiological changes in the gut, including redox dyshomeostasis, resulting from central neuropathology. Our study aimed to investigate the mechanisms underlying gut redox dyshomeostasis and assess the effects of D-galactose, which is known to benefit gut redox homeostasis and alleviate cognitive deficits in this model. Duodenal rings isolated from STZ-icv animals and control groups were subjected to a prooxidative environment using 2,2′-azobis(2-amidinopropane) dihydrochloride (AAPH) or H_2O_2 with or without D-galactose in oxygenated Krebs buffer ex vivo. Redox homeostasis was analyzed through protein microarrays and functional biochemical assays alongside cell survival assessment. Structural equation modeling and univariate and multivariate models were employed to evaluate the differential response of STZ-icv and control samples to the controlled prooxidative challenge. STZ-icv samples showed suppressed expression of catalase and glutathione peroxidase 4 (GPX4) and increased baseline activity of enzymes involved in H_2O_2 and superoxide homeostasis. The altered redox homeostasis status was associated with an inability to respond to oxidative challenges and D-galactose. Conversely, the presence of D-galactose increased the antioxidant capacity, enhanced catalase and peroxidase activity, and upregulated superoxide dismutases in the control samples. STZ-icv-induced gut dysfunction is characterized by a diminished ability of the redox regulatory system to maintain long-term protection through the transcription of antioxidant response genes as well as compromised activation of enzymes responsible for immediate antioxidant defense. D-galactose can exert beneficial effects on gut redox homeostasis under physiological conditions.
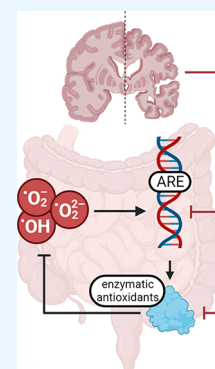
INTRODUCTION

A growing body of evidence suggests that bidirectional communication between the gut and the brain may play an important role in the development and progression of neurodegenerative disorders, including Alzheimer's disease (AD).[1] The gastrointestinal (GI) tract serves as a potential gateway for toxins, amyloidogenic proteins, and microorganisms due to its large surface area, vast number of intraluminal microbes, and the significant vulnerability of the GI barrier.[2,3] Moreover, the gut acts as the body's largest immune organ, capable of initiating and maintaining systemic inflammation and oxidative stress, which can have significant impacts on overall metabolic homeostasis.[4−6] As a result, these processes can lead to neuroinflammation, insulin resistance, and ultimately neurodegeneration.[7−12] The communication from the brain to the gut plays a vital role in preserving the structural and functional integrity of the GI barrier.[5,13,14] As a result, even when neurodegeneration primarily affects the central nervous system (CNS), the GI barrier's integrity will inevitably be compromised, leading to a harmful pathophysio-logical positive feedback loop between the brain and the gut. Understanding the pathophysiological changes in the GI tract related to neuropathological changes in the brain is a crucial area of research that offers an opportunity to slow down the progression of neurodegenerative disorders by preventing chronic inflammation and oxidative stress caused by altered GI homeostasis and the breakdown of the gut-brain axis.

In transgenic animal models of AD, it is common to observe physiological changes in the GI tract before observing any pathological changes in the brain.[15−17] This sequence of events makes it difficult to study the GI consequences of localized neurodegeneration in the CNS. On the other hand, brain-first
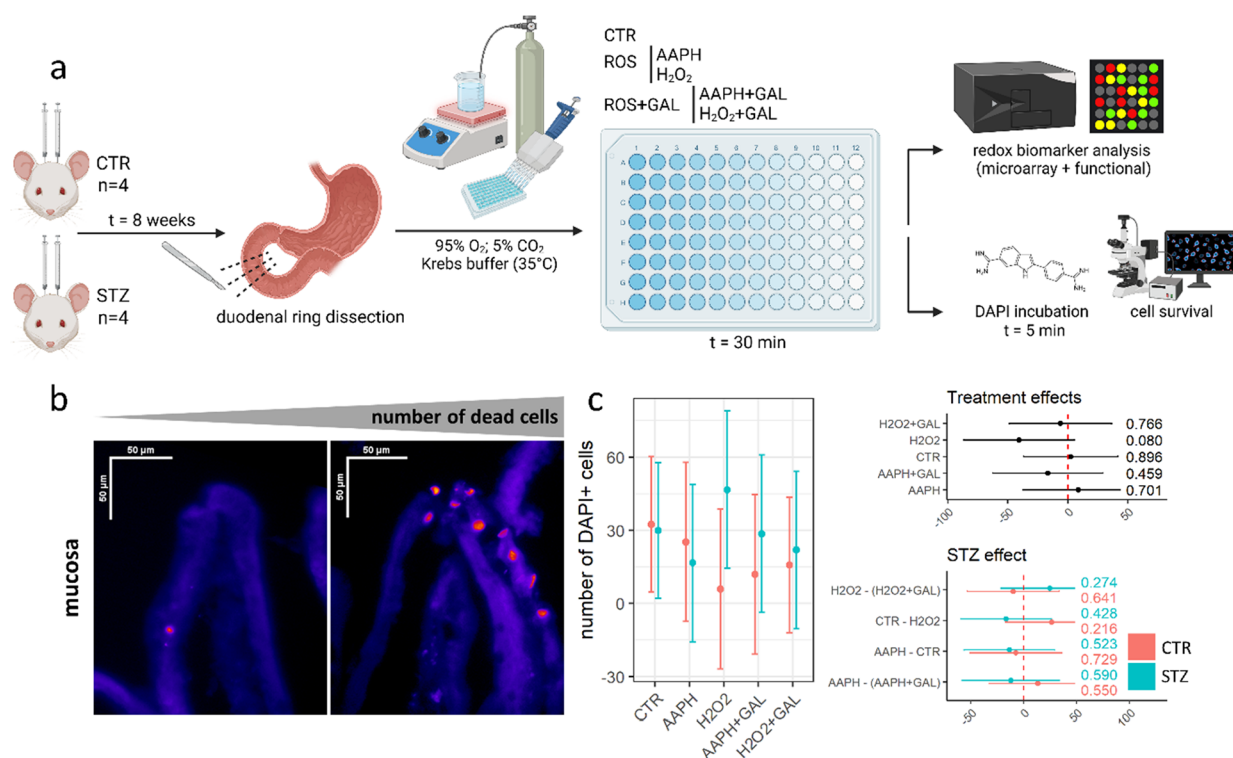
Figure 1. Experimental design and analysis of cell survival. Experimental design: Duodenal rings isolated from the rat model of sporadic Alzheimer's disease and respective controls were incubated in the oxygenated Krebs buffer simulating prooxidative conditions with and without the presence of D-galactose. Cell survival was analyzed by quantifying 4′,6-diamidino-2-phenylindole (DAPI) after 5 min of incubation with DAPI-containing Krebs solution indicating the loss of membrane integrity of cells. Remaining samples were snap-frozen in liquid nitrogen and stored for subsequent analysis of enzymatic activity and redox biomarkers. (a) Representative photomicrograph of the DAPI signal with dead cells shown in warm colors (*Fire* Look-Up Table); (b) quantification of dead cells with group estimates (left) and effect sizes (right) accompanied by 95% confidence intervals and *p*-values; and (c) treatment effects reported as contrasts of CTR. AAPH, 2,2′-Azobis(2-amidinopropane) dihydrochloride incubation; H_2O_2, hydrogen peroxide incubation; ROS, reactive oxygen species (prooxidative environment); GAL, D-galactose.

nontransgenic animal models, which involve the targeted delivery of toxic substances (e.g., amyloid β,[18] streptozotocin (STZ),[19] colchicine,[20] and okadaic acid[21]) that mimic AD-related neuropathology to the CNS, provide an opportunity to investigate the one-way disruption of the gut−brain axis.[22−25] These models offer invaluable insights into how localized neurodegeneration impacts the structural and functional integrity of the gut. One of the most extensively studied and well-established brain-first models of sporadic AD is the rat model generated by intracerebroventricular administration of the diabetogenic toxin streptozotocin (STZ-icv).[19,26] Based on the evidence accumulated over the last 30 years, the STZ-icv model recapitulates key behavioral and neuropathological hallmarks of AD.[19] Following STZ administration, the animals develop the insulin-resistant brain state associated with mitochondrial dysfunction and glucose hypometabolism,[27,28] oxidative stress,[29] neuroinflammation,[30,31] neuropathological changes related to accumulation of amyloid β and hyper-phosphorylated tau,[32,33] chronic and progressive cognitive deficits, and circadian dysrhythmia.[19,34,35] The precise molecular mechanisms through which STZ induces pathological changes reminiscent of AD remain incompletely understood. Nevertheless, it appears that the actions of STZ are mediated by its uptake through the glucose transporter 2 (GLUT2),[36] followed by harmful effects on the targeted cells, most likely through the alkylation of DNA by its methyl nitrosourea component.[37,38] This DNA damage, in turn, triggers poly adenosine diphosphate-ribosylation and results

in a decrease in nicotinamide adenine dinucleotide and adenosine triphosphate (ATP) levels.[38] Furthermore, it has been demonstrated that STZ can directly release nitric oxide (NO) and induce mitochondrial dysfunction.[38,39] Although various other speculative mechanisms have been explored, they all ultimately lead to significant disruption of cellular energy and redox balance, resulting in the loss of cellular function and, ultimately, cell death.[40] Interestingly, dysfunctional gut−brain axis and pathophysiological changes in the gut were also reported in this model, indicating that it represents a valid platform for investigating the GI consequences of neurodegeneration affecting the CNS. The STZ-icv gut is characterized by violated structural and functional properties of the GI barrier,[41] distorted secretion and constitution of gut mucus,[24] redox dyshomeostasis,[22,42] and altered absorption.[43]

In this study, we focused on redox homeostasis as oxidative stress plays a key etiopathogenetic role in neurodegenerative diseases,[9,44−46] including AD.[8,47] Multiple studies utilizing complementary molecular markers have demonstrated increased levels of oxidative stress in diverse brain regions of individuals with Alzheimer's disease, thereby offering robust evidence supporting the involvement of oxidative stress in AD. For example, AD has been associated with increased levels of brain and cerebrospinal fluid protein carbonyls, 4-hydroxynonenal (4-HNE), 3-nitrotyrosine, 8-hydroxyguanosine, malondialdehyde, and decreased activity of antioxidant enzymes such as superoxide dismutase and catalase.[47−58] Crucially, mechanistic studies have revealed that oxidative
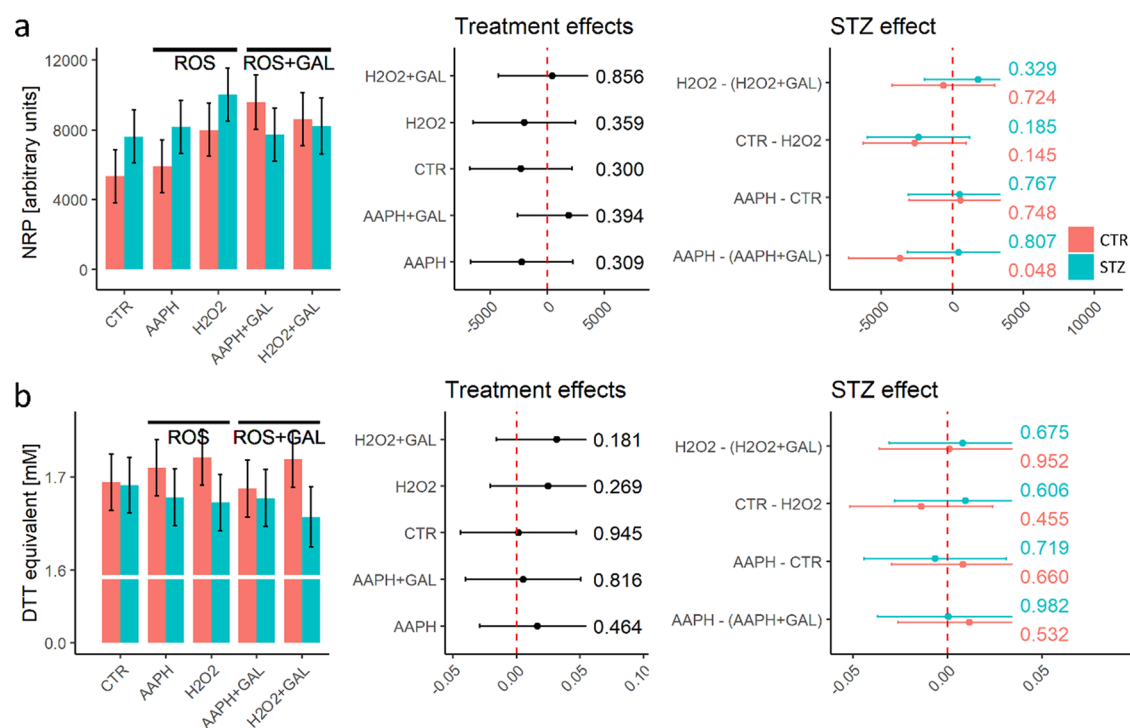
Figure 2. Analysis of antioxidant capacity. NRP signal group estimates (left) and effect sizes (right) (a). ABTS signal group estimates (left) and effect sizes (right) (b). The error bars in the bar graphs represent standard errors, while for effect size estimates, 95% confidence intervals are provided. Effect sizes were presented in two ways: as contrasts of groups (CTR vs STZ) at the levels of treatments (CTR/AAPH/H_2O_2/AAPH + GAL/H_2O_2 + GAL), and as contrasts of the control and experimental conditions (CTR vs AAPH/H_2O_2/AAPH + GAL/H_2O_2 + GAL) for CTR and STZ groups individually. *P*-values are reported alongside the model-derived estimates. AAPH, 2,2′-Azobis(2-amidinopropane) dihydrochloride incubation; H_2O_2, hydrogen peroxide incubation; ROS, reactive oxygen species (prooxidative environment); GAL, D-galactose.

stress is not merely a result of other pathophysiological processes; rather, it actively contributes as a causative factor, serving as a connecting link between various mechanisms outlined in the proposed hypotheses of Alzheimer's disease.[8,47,51,53,56]

Considering the vital function of redox homeostasis in preserving gut function and the integrity of the GI barrier,[4] which consequently acts as a crucial controller of overall body redox balance,[4,59] the main focus of this study was to employ an ex vivo approach to investigate the underlying mechanisms behind the observed redox dyshomeostasis in the gut of the STZ-icv model. The aim was to subject intestinal rings to a controlled oxidative environment and assess their ability to withstand an exogenous oxidative challenge, which necessitates functional redox homeostasis. The secondary goal of the study was to investigate the effects of D-galactose on redox homeostasis in the STZ-icv gut. This was motivated by previous findings that while parenteral D-galactose administration has been linked to oxidative stress and cognitive decline,[60] chronic oral D-galactose treatment has shown promising results in preventing and alleviating cognitive deficits in the STZ-icv model.[28,61−63] Additionally, orally administered D-galactose has been found to have beneficial effects on redox homeostasis both in the GI tract[64] and the brain.[65]

■ RESULTS

To evaluate the impact of prooxidative environments (AAPH and H_2O_2) and the potential protective effects of D-galactose on both CTR and STZ intestinal cells, we initiated our analysis by examining the survival of mucosal cells (Figure 1A,B). The

number of dead cells under normal conditions (Krebs buffer) was comparable between those of the control group (CTR) and the STZ-treated group (Figure 1C). The only instance in which a noticeable distinction in cell survival between the CTR and STZ tissue was observed was during incubation with H_2O_2. This resulted in reduced estimates of the number of dying cells in the CTR group and decreased survival in the STZ mucosa (Figure 1C). The reduced survival of STZ cells showed partial improvement when coincubated with D-galactose, with a 2-fold reduction in cell death observed in the case of STZ-icv duodenal rings coincubated with D-galactose. However, it is essential to highlight that these effects were associated with considerable uncertainty, as indicated by the large standard errors, and therefore, further confirmation is warranted through additional biological replications (see Figure 1C).

In STZ tissue, the nitrocellulose redox permanganometry (NRP) biomarker, which indicates total antioxidant capacity,[66] showed no significant response. However, in the control group, the NRP levels were higher in the pro-oxidative environment regardless of the presence of D-galactose (Figure 2A). Interestingly, the 2,2′-azino-bis(3-ethylbenzothiazoline-6-sulfonic acid) (ABTS) assay indicated a reduced overall antioxidant capacity in the STZ tissue, which was not improved by coincubation with D-galactose (Figure 2B). It is worth noting that, except for the increased antioxidant capacity (NRP) observed in the control tissues incubated with D-galactose in the presence of 2,2′-Azobis(2-amidinopropane) dihydrochloride (AAPH), both biomarkers of total antioxidant capacity indicated that the effects were modest and
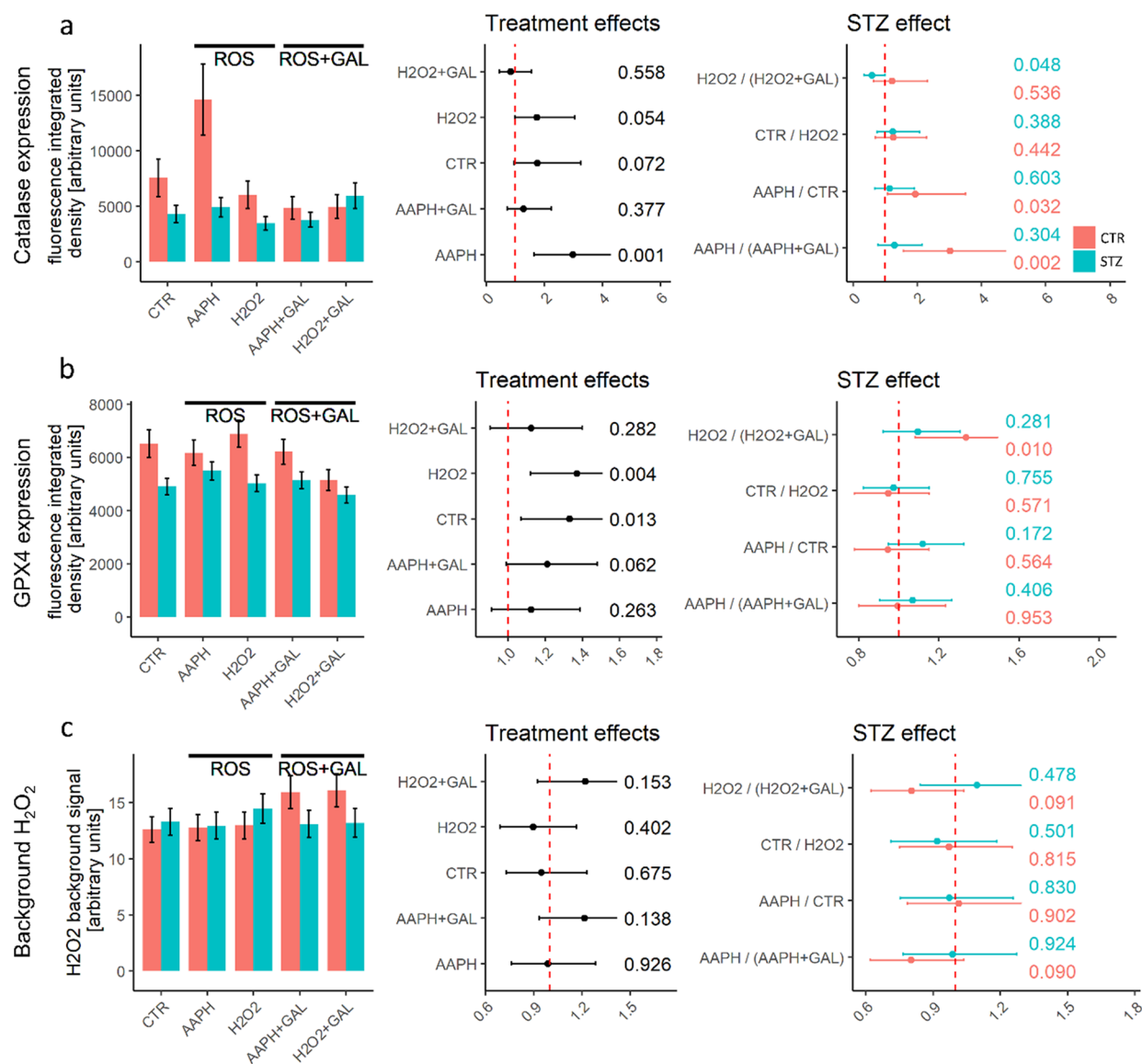
Figure 3. Expression of catalase (CAT) and glutathione peroxidase (GPX4) and baseline H_2O_2. CAT signal group estimates (left) and effect sizes (right) (a). GPX4 signal group estimates (left) and effect sizes (right) (b). Background H_2O_2 signal group estimates (left) and effect sizes (right) (c). The error bars in the bar graphs represent standard errors, while for effect size estimates, 95% confidence intervals are provided. Effect sizes were presented in two ways—as contrasts of groups (CTR vs STZ) at the levels of treatments (CTR/AAPH/H_2O_2/AAPH + GAL/H_2O_2 + GAL) and as contrasts of the control and experimental conditions (CTR vs AAPH/H_2O_2/AAPH + GAL/H_2O_2 + GAL) for CTR and STZ groups individually. *P*-values are reported alongside the model-derived estimates. AAPH, 2,2′-Azobis(2-amidinopropane) dihydrochloride incubation; H_2O_2, hydrogen peroxide incubation; ROS, reactive oxygen species (prooxidative environment); GAL, D-galactose.

accompanied by considerable uncertainty estimates (Figure 2A,B).

Subsequently, we investigated the H_2O_2 pathway, which plays a crucial role in redox signaling. In the CTR, the presence of AAPH led to a significant induction of CAT expression, while the coincubation with D-galactose prevented this response. In the STZ tissue, CAT expression remained relatively stable across all conditions except when H_2O_2 and D-galactose were present. In this case, D-galactose prevented H_2O_2-induced suppression and stimulated the expression of CAT (Figure 3a). The expression of GPX4 was consistently decreased in the STZ group across all conditions. In the control group, the presence of D-galactose resulted in reduced levels of GPX4 expression when H_2O_2 was present. However, in the STZ tissue, the effects of D-galactose on GPX4 expression were absent (Figure 3B). The background H_2O_2

signal in the STZ group remained unchanged in all conditions, while in the controls, it increased with the presence of D-galactose (Figure 3C).

CAT activity showed no significant changes across conditions in the STZ group, indicating the reduced responsiveness of STZ cells, whereas in the control group, CAT was activated in response to the oxidative environment, and the presence of D-galactose further stimulated CAT activity in the AAPH + GAL group (Figure 4A). Interestingly, the activation of peroxidases demonstrated a similar level of responsiveness in both the CTR and STZ tissues, with the highest activation observed in the presence of D-galactose in both groups. The only distinction between the CTR and STZ was observed when the tissue was incubated with H_2O_2, where the activation of the peroxidase system was exclusively observed in the STZ group (Figure 4B). The absence of
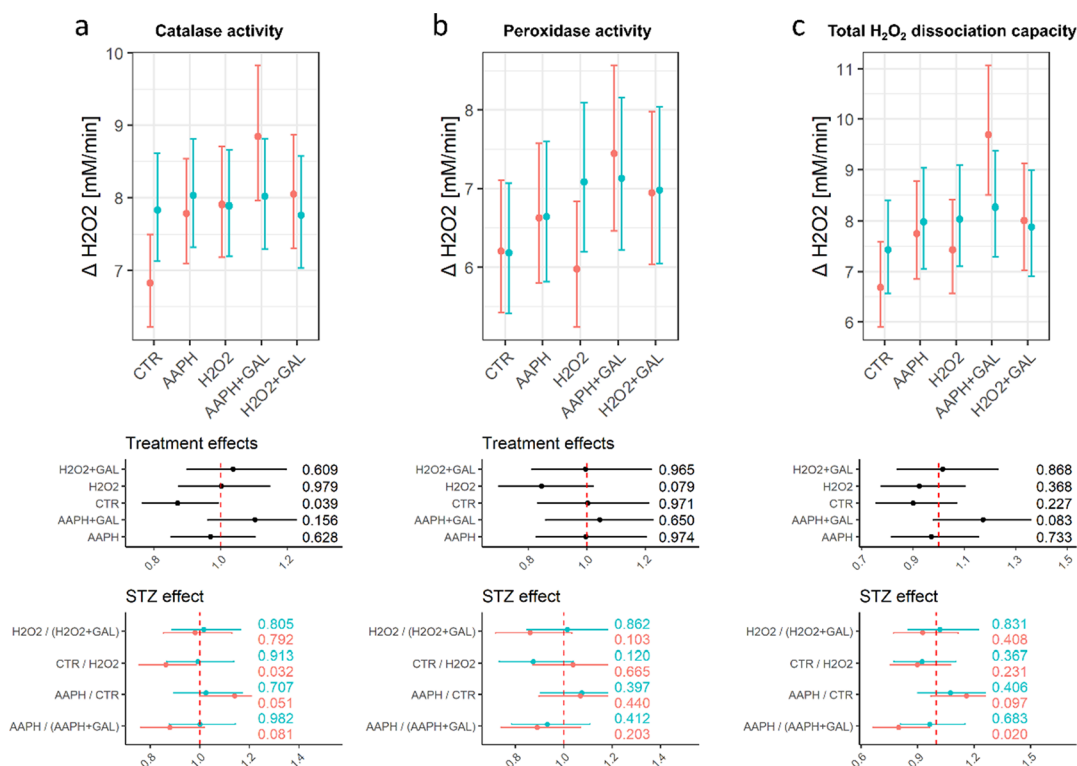
Figure 4. Total H_2O_2 dissociation capacity and the activity of catalase and peroxidases. Catalase activity group estimates (top) and effect sizes (bottom) (a). Peroxidase activity group estimates (top) and effect sizes (bottom) (b). Total H_2O_2 dissociation capacity group estimates (top) and effect sizes (bottom) (c). Effect sizes were presented in two ways—as contrasts of groups (CTR vs STZ) at the levels of treatments (CTR/AAPH/ H_2O_2/AAPH + GAL/H_2O_2 + GAL) and as contrasts of the control and experimental conditions (CTR vs AAPH/H_2O_2/AAPH + GAL/H_2O_2 + GAL) for CTR and STZ groups individually. *P*-values are reported alongside the model-derived estimates. AAPH, 2,2′-Azobis(2-amidinopropane) dihydrochloride incubation; H_2O_2, hydrogen peroxide incubation; ROS, reactive oxygen species (prooxidative environment); GAL, D-galactose.
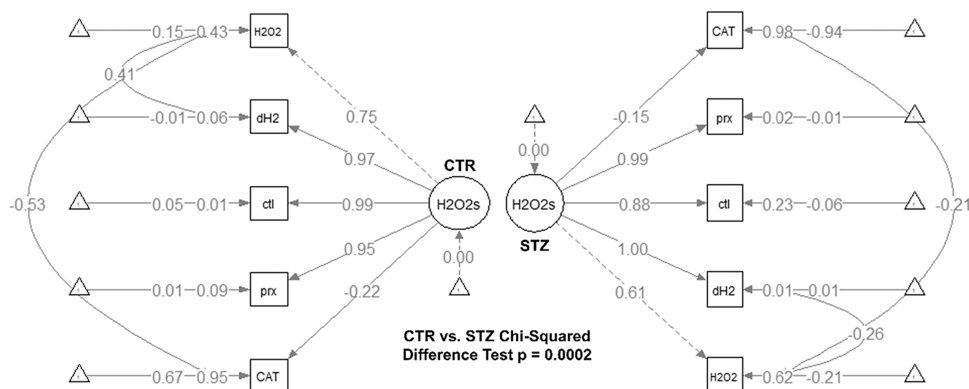

Figure 5. Hydrogen peroxide system structural equation model. Structural equation models (SEMs) were obtained with standardized loadings for the CTR (left) and STZ (right). Manifest variables are depicted as squares, while latent variables are shown as circles. CTR, control; STZ, streptozotocin; H_2O_2, background H_2O_2; dH2, H_2O_2 dissociation capacity; ctl, catalase activity; prx, glutahione peroxidase 4 activity; CAT, catalase expression; ROS, reactive oxygen species (prooxidative environment); GAL, D-galactose.

CAT activation and the increased activity of peroxidases in response to H_2O_2 exposure point to a compensatory mechanism employed by STZ tissue to maintain redox homeostasis. This suggests that the STZ tissue relies on the activation of alternative systems for removing H_2O_2 to counterbalance the deficient CAT activity. The total H_2O_2 dissociation capacity exhibited a similar pattern to that of CAT activation, indicating once again the diminished responsiveness of the STZ tissue, while the greatest stimulation of H_2O_2 removal systems was observed in the CTR tissue exposed to AAPH and D-galactose (Figure 4C).

Comparative analysis using SEMs revealed significant alterations in the H_2O_2 signaling system in the STZ tissue (χ^2 p = 0.0002) (Figure 5). The SEM results indicated that H_2O_2 signaling in STZ tissue relied less on CAT activation and CAT expression to regulate baseline H_2O_2 levels. Additionally, the covariance between the activation of the H_2O_2 removal system and baseline H_2O_2 was reversed in the STZ group, suggesting a potential decrease in the capacity of protective systems and/or an increased impact of H_2O_2-generating systems.
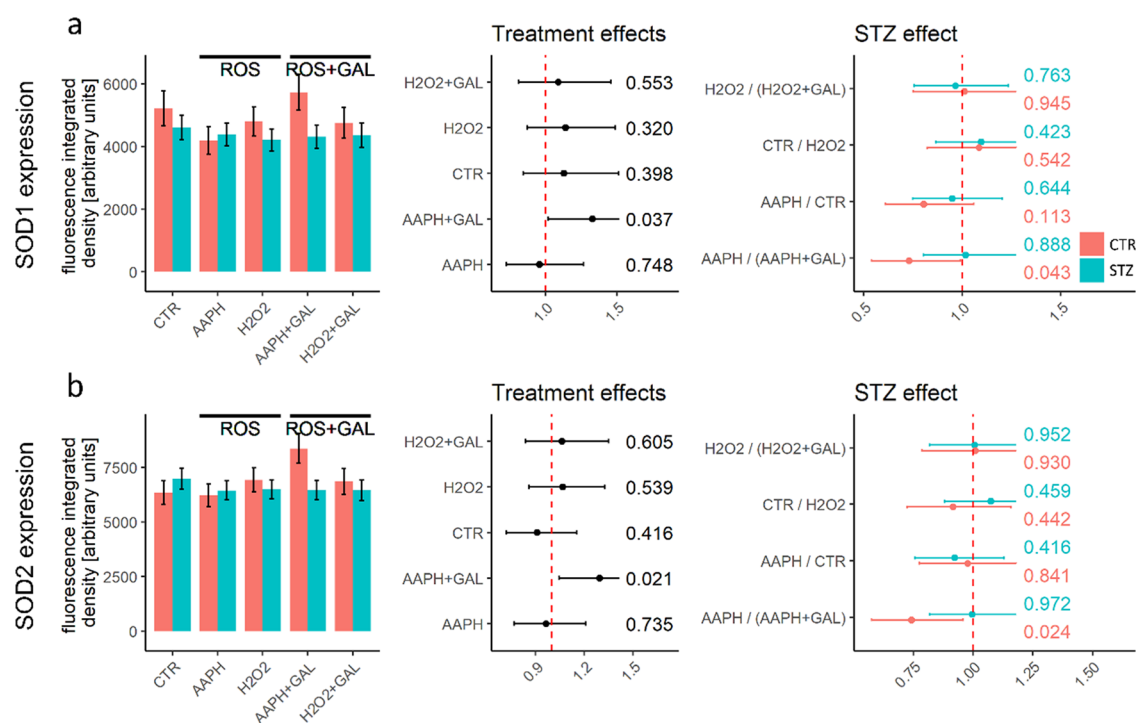
Figure 6. Expression of superoxide dismutase 1 (SOD1) and superoxide dismutase 2 (SOD2). SOD1 signal group estimates (left) and effect sizes (right)(a). SOD2 signal group estimates (left) and effect sizes (right)(b). The error bars in the bar graphs represent standard errors, while for effect size estimates, 95% confidence intervals are provided. Effect sizes were presented in two ways—as contrasts of groups (CTR vs STZ) at the levels of treatments (CTR/AAPH/H_2O_2/AAPH + GAL/H_2O_2 + GAL), and as contrasts of the control and experimental conditions (CTR vs AAPH/H_2O_2/AAPH + GAL/H_2O_2 + GAL) for CTR and STZ groups individually. *P*-values are reported alongside the model-derived estimates. AAPH, 2,2′-Azobis(2-amidinopropane) dihydrochloride incubation; H_2O_2, hydrogen peroxide incubation; ROS, reactive oxygen species (prooxidative environment); GAL, D-galactose.

Another important aspect of maintaining homeostatic control involves the regulation of the turnover of $O_2^{\cdot-}$ and conversion into H_2O_2 through the SOD system. In the control group, the expression of SOD1 decreased when incubated with AAPH, whereas coincubation with AAPH and D-galactose led to increased expression of both SOD1 and SOD2 (Figure 6A,B). The presence of H_2O_2 had no impact on the expression of SOD1 and SOD2, regardless of the presence of D-galactose in the control group. In contrast, the STZ samples again showed reduced responsiveness to environmental changes, as evidenced by the consistent expression levels of SOD1 and SOD2 across all conditions (Figure 6A,B).

At the baseline, SOD1 activity and total $O_2^{\cdot-}$ dissociation capacity were higher in the STZ samples compared to the controls, indicating an increased demand for $O_2^{\cdot-}$ removal in the former group (Figure 7A−C)). In the control group, the presence of either AAPH or H_2O_2 led to an increase in the SOD1 activity, while the SOD2 activity remained unchanged. The addition of D-galactose had no effect on the SOD1 activity, the SOD2 activity, or the total $O_2^{\cdot-}$ dissociation capacity of the control samples. However, when D-galactose was introduced in the presence of H_2O_2, it reduced the level of activation of cytoplasmic SOD and increased the level of activation of mitochondrial SOD.

The SEM analysis revealed a significant disturbance of the SOD system in the STZ samples (χ^2 p = 0.002). When the STZ samples were compared to the controls, it became evident that the SOD system in the former was more reliant on the activity of mitochondrial SOD, as indicated by SEM standardized estimates (Figure 8).

At the baseline, the STZ samples showed a reduction in the expression of nNOS, with a level of change similar to that achieved in the control samples when exposed to a prooxidative environment (Figure 9A). In the control group, the expression of nNOS decreased when the samples were incubated with AAPH or H_2O_2, and the addition of D-galactose had no impact on this expression. However, in the STZ samples, the expression of nNOS remained comparable across all conditions (Figure 9A). Surprisingly, despite the differences in nNOS expression, there were only minimal changes in NO levels across the various conditions in both groups (Figure 9B). Finally, TBARS levels were comparable across groups and conditions reflecting modest changes in total antioxidant capacity biomarkers (Figure 2A,B).

Using nonlinear dimensionality reduction through UMAP, we observed that CTR and STZ samples could be differentiated based on redox biomarkers measured in this study under normal control conditions and when exposed to prooxidative conditions, especially with AAPH (Figure 10A). However, the distinction between the two groups became less apparent in the presence of D-galactose. This attenuation of sample dissimilarity could be attributed to the interaction between the effects of STZ and D-galactose reflected in normalization of the activity of enzymes responsible for $O_2^{\cdot-}$ and H_2O_2 homeostasis. Another possibility is that the decrease in dissimilarity was mainly influenced by the effects of D-galactose in the CTR and its absence in the STZ group. This is indicated by the lack of distinction between the samples treated with galactose and those untreated in the STZ group (Figure 10B).
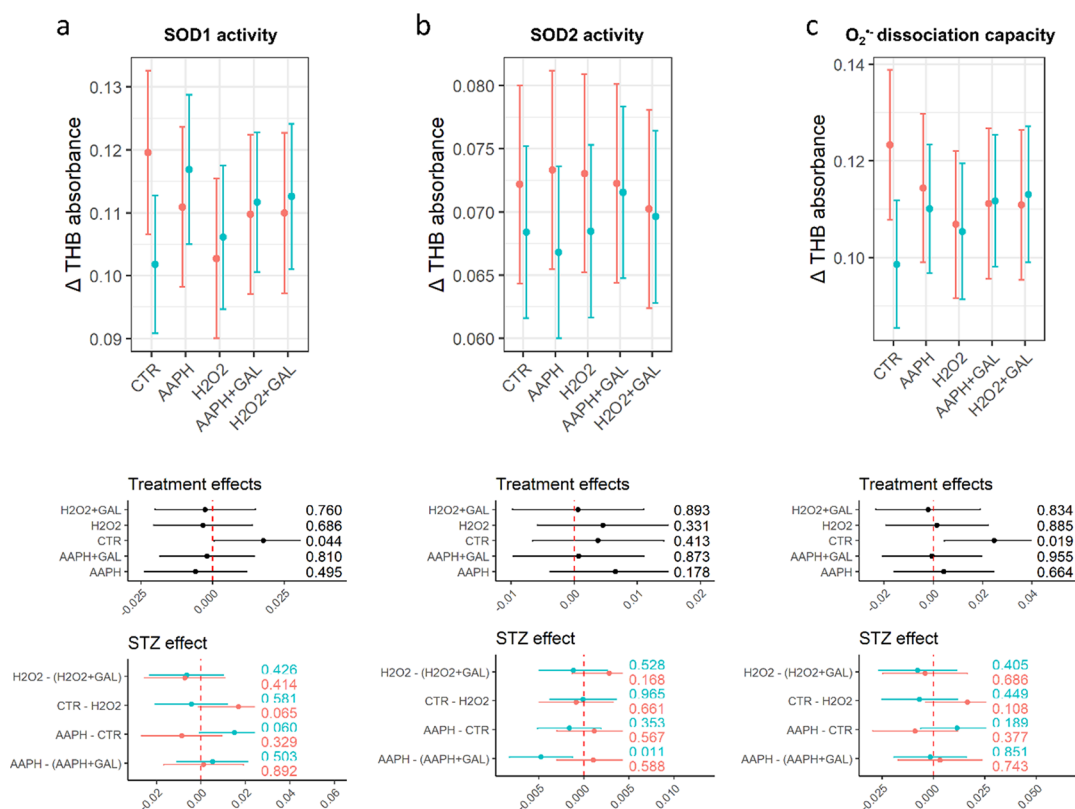
Figure 7. Total superoxide dissociation capacity and activity of superoxide dismutase 1 (SOD1) and superoxide dismutase 2 (SOD2). The estimates of THB absorbance difference are inversely proportional to the removal of superoxide radicals. SOD1 activity group estimates (top) and effect sizes (bottom)(a). SOD2 activity group estimates (top) and effect sizes (bottom)(b). Total superoxide dissociation capacity group estimates (top) and effect sizes (bottom)(c). Effect sizes were presented in two ways—as contrasts of groups (CTR vs STZ) at the levels of treatments (CTR/AAPH/H_2O_2/AAPH + GAL/H_2O_2 + GAL), and as contrasts of the control and experimental conditions (CTR vs AAPH/H_2O_2/AAPH + GAL/H_2O_2 + GAL) for CTR and STZ groups individually. *P*-values are reported alongside the model-derived estimates. AAPH, 2,2′-Azobis(2-amidinopropane) dihydrochloride incubation; H_2O_2, hydrogen peroxide incubation; ROS, reactive oxygen species (prooxidative environment); GAL, D-galactose.
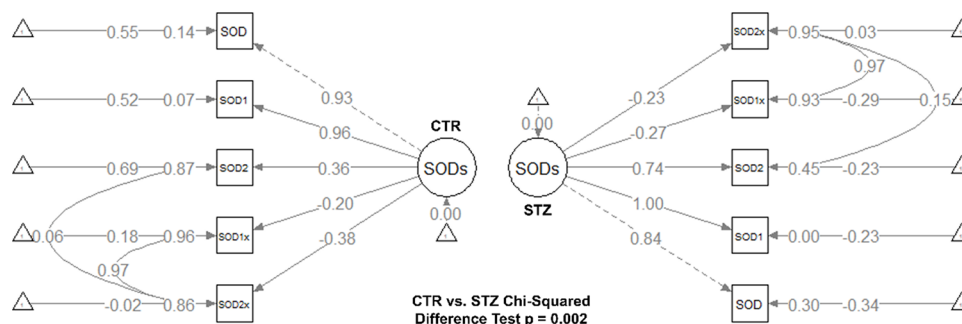

Figure 8. Superoxide dismutase structural equation model. Structural equation models (SEMs) with standardized loadings for the CTR (left) and STZ (right). Manifest variables are depicted as squares, while latent variables are shown as circles (d). Error bars representing 95% confidence intervals are provided. *P*-values are reported alongside the model-derived estimates. CTR, control; STZ, streptozotocin; SOD, total superoxide dissociation capacity; SOD1, SOD1 activity; SOD2, SOD2 activity; SOD1x, expression of SOD1; SOD2x, expression of SOD2; ROS, reactive oxygen species (prooxidative environment); GAL, D-galactose.

■ DISCUSSION

The presented results offer invaluable insights into the potential mechanisms underlying the disturbance of redox balance in the gastrointestinal system of the STZ-icv rat model of AD.[22] Collectively, these findings suggest that the STZ-induced gut dysfunction is characterized by a reduced ability of the redox regulatory system to maintain long-term protection through the transcription of genes involved in the antioxidant response as well as a compromised activation of enzymes responsible for immediate antioxidant defense. Baseline expression of CAT and GPX4 showed decreased levels in the STZ samples. The tested conditions (oxidative environment; D-galactose) had no significant effect on the expression of the four redox-related proteins (CAT, SOD1, SOD2, and GPX4) in STZ tissue, with one exception. Notably, CAT expression showed an increase when STZ rings were exposed to H_2O_2 in the presence of D-galactose. In contrast, the presence of oxidants or D-galactose did affect the expression of
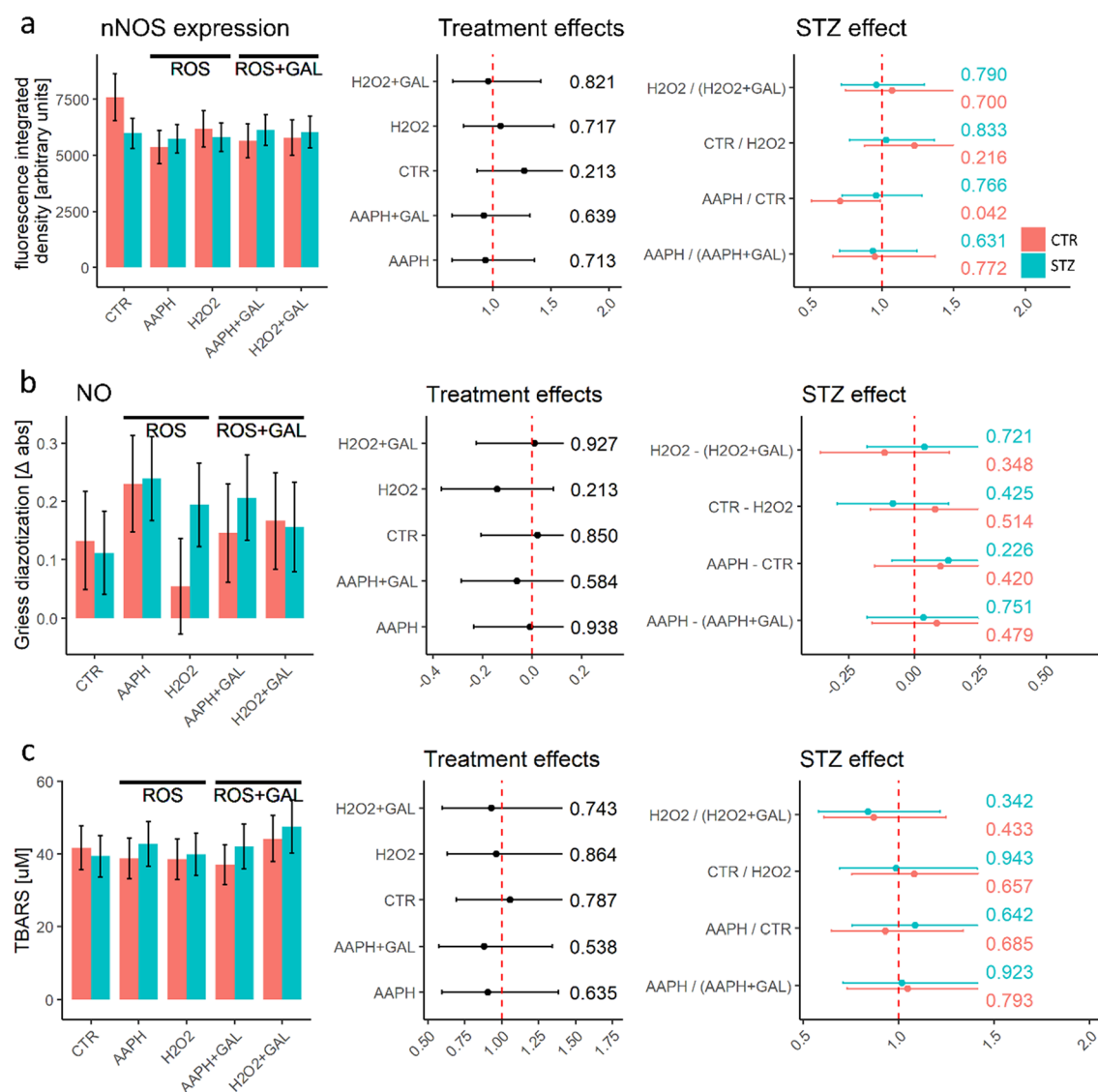
Figure 9. Expression of neuronal nitric oxide synthase (nNOS) and quantification of nitrites and thiobarbituric acid reactive substances (TBARS). nNOS expression group estimates (left) and effect sizes (right) (a). Nitrite concentration group estimates (left) and effect sizes (right) (b). TBARS concentration group estimates (left) and effect sizes (right) (c). The error bars in the bar graphs represent standard errors, while for effect size estimates, 95% confidence intervals are provided. Effect sizes were presented in two ways—as contrasts of groups (CTR vs STZ) at the levels of treatments (CTR/AAPH/H_2O_2/AAPH + GAL/H_2O_2 + GAL), and as contrasts of the control and experimental conditions (CTR vs AAPH/H_2O_2/AAPH + GAL/H_2O_2 + GAL) for CTR and STZ groups individually. P-values are reported alongside the model-derived estimates. AAPH, 2,2′-Azobis(2-amidinopropane) dihydrochloride incubation; H_2O_2, hydrogen peroxide incubation; ROS, reactive oxygen species (prooxidative environment); GAL, D-galactose.

CAT, GPX4, and SODs in the control group. Due to the relatively short incubation times (30 min), definitive conclusions regarding protein expression cannot be drawn, and it is possible that the expression of the mentioned proteins in the STZ tissue was not entirely absent but rather delayed. Nevertheless, the data strongly suggest a lack of transcriptional/translational reactivity to oxidative stimuli and/or D-galactose in the STZ samples. The lack of redox reactivity in STZ duodenal rings was also evident in the impaired activation of enzymes crucial for immediate antioxidant defense, specifically CAT (and total H_2O_2 dissociation capacity), as well as SOD1 (and total $O_2^{·−}$ conversion capacity). At the baseline, the activity of both CAT and SOD1 was elevated in STZ tissue, suggesting heightened stress on the redox system responsible for removing $O_2^{·−}$ and H_2O_2. When exposed to oxidants, control tissue samples demonstrated a compensatory

activation of CAT and SOD1, whereas duodenal rings from STZ-icv animals exhibited either absent (CAT) or reversed (SOD1) responses. The mechanisms behind the observed effects have yet to be fully understood. One possible explanation is that the $O_2^{·−}$ and H_2O_2 removal systems in the STZ gut are already functioning at their maximum activation due to a constitutively increased electrophilic tone.[22] Alternatively, the absence of a response in the STZ tissue samples could be attributed to altered cellular pathways responsible for modulating the activation of antioxidant enzymes. For instance, previous research has indicated that protein kinases can swiftly regulate CAT activity,[67] and the mammalian target of rapamycin (mTOR) directly phosphorylates and activates SOD1.[68] Further investigation is needed to clarify the exact mechanisms underlying these findings. Nrf2 stands out as a vital signaling pathway that governs the control
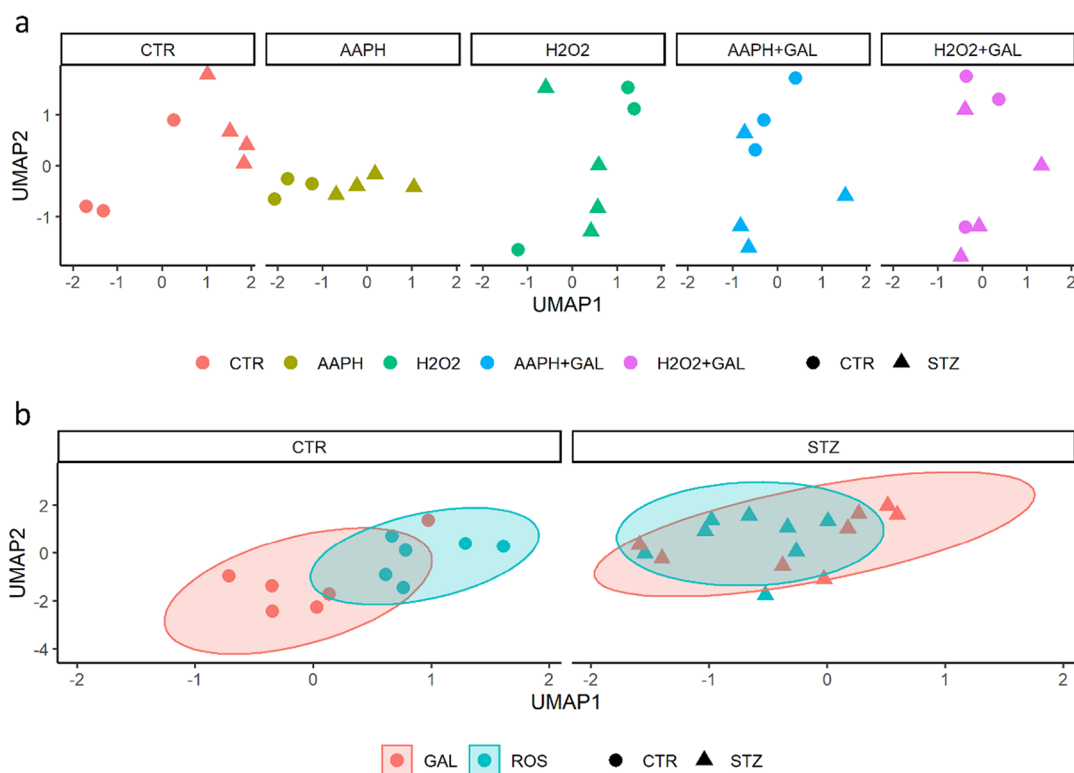
Figure 10. Nonlinear dimensionality reduction based on a uniform manifold approximation and projection (UMAP). Positions in the UMAP biplot based on treatment conditions (a). Representation of UMAP dissimilarity of CTR and STZ samples with or without D-galactose treatement. ROS, reactive oxygen species (prooxidative environment); GAL, D-galactose.

of cellular antioxidant defense capacity, especially in response to nutrients and oxidative stress.[69−73] Given the reduced ability of STZ cells to react to a pro-oxidative environment by boosting their antioxidant mechanisms, it is imperative for future research to investigate whether the absence of this compensatory response in STZ cells could be linked to the dysregulation of Nrf2 and its associated pathways. In both groups, the reactivity of SOD2 activity was minimal, suggesting that its modulation was not a significant factor in the response to coincubation with oxidants and D-galactose. However, the peroxidase system showed involvement in the response, and intriguingly, its reactivity and responsiveness were preserved in the STZ group. In fact, the total peroxidase activity showed a difference only when the samples were incubated with H_2O_2, suggesting that its overactivation might have been a compensatory response to the insufficient reactivity of catalase in this context. It is crucial to emphasize that the only condition under which a significant difference in the survival of mucosal cells was noticed is during incubation with H_2O_2 without D-galactose. The results indicate that the mucosa in the STZ group is more susceptible to H_2O_2-induced damage, possibly due to the reduced reactivity of the redox response. However, it is essential to consider the potential biases introduced by the decreased survival of STZ cells. First, the activity of redox-related enzymes might have been influenced by molecular signaling triggered by dying cells. For instance, in a study involving dextran sulfate sodium-induced death of colonocytes, the loss of CAT and SOD1 activity was observed.[74] A second concern is the potential introduction of attrition bias due to the loss of vulnerable cells, leaving only the least susceptible cells available for analysis. As a result, caution

should be exercised when interpreting the response to H_2O_2 based on the reported results.

Co-incubation with D-galactose showed positive effects on redox homeostasis when cells were exposed to a prooxidative environment. However, this response was observed only in the control samples. In the control samples exposed to a prooxidative environment caused by AAPH, D-galactose enhanced the antioxidant capacity (NRP) and prevented the upregulation of CAT expression induced by AAPH. This effect may be attributed to an increase in the activity of both CAT and peroxidases, leading to approximately 45% greater total H_2O_2 dissociation capacity. Interestingly, while D-galactose did not affect the activity of SODs, it upregulated the expression of both SOD1 and SOD2, possibly providing long-term protection against AAPH-induced damage. When control samples were exposed to a prooxidative environment generated by H_2O_2, the effects on CAT activity and expression were not observed. Instead, D-galactose activated peroxidases and reduced the expression of GPX4, suggesting the activation of an alternative adaptive response. Together, the results indicate that D-galactose has the capacity to positively impact gut redox homeostasis. These findings are consistent with an in vivo study conducted on rats, where the acute oral administration of D-galactose showed beneficial effects on the redox homeostasis of the small intestine.[64] Furthermore, these results provide additional evidence supporting the notion that D-galactose's protective effects on the gut, such as protection against ionizing radiation,[75] may be attributed to its ability to modulate redox homeostasis.[76]

The results presented here underscore D-galactose's ability to deliver positive effects at low doses, which stands in stark contrast to the widely recognized harmful consequences of D-

galactose when administered intravenously at excessively high doses that simulate oxidative stress and aging in different experimental models[60,77−80] via molecular mechanisms that still need to be completely understood.[65,81] The findings from this study provide evidence for the hypothesis that D-galactose can induce hormetic effects, where the extent of tissue exposure plays a pivotal role in determining whether its actions in cells are beneficial or harmful.[64,65,76,82] The STZ samples showed an attenuated response to D-galactose treatment. The only noticeable effect of D-galactose in the STZ duodenal rings was an increase in mucosal cell survival, coupled with an upregulation of CAT expression when the samples were exposed to H_2O_2. The lack of response of STZ samples to D-galactose in the pro-oxidative environment is evident from the absence of spatial distinction in UMAP. The mechanistic explanation for the lack of response of STZ samples to D-galactose treatment remains elusive. However, previous experiments have indicated that the beneficial effects of D-galactose on redox homeostasis rely on the utilization of reductive equivalents, such as low-molecular-weight thiols (LMWT) and reduced nicotinamide adenine dinucleotide phosphate (NADPH),[64] possibly due to its hormetic effects.[65] This suggests that the reduced concentration of LMWT in the duodenum, as observed in the STZ-icv model of AD,[22] could potentially contribute to the absence of a positive response to D-galactose treatment observed in this study.

Previous experiments have revealed that duodenal goblet cells in the STZ-icv rat model of AD do not respond to cholinergic stimulation for mucus secretion.[24] This study builds upon those findings by demonstrating that the GI tracts in STZ-icv rats also exhibit reduced responsiveness to an oxidative environment and exposure to D-galactose. Consequently, this suggests that the GI tracts of STZ-icv rats may generally be considered unresponsive to both internal and external stimuli.

To gain a deeper understanding of the underlying pathophysiological processes in the gut resulting from central neurodegeneration, future experiments should focus on investigating how changes in the CNS contribute to the observed unresponsive behavior in GI cells. This aspect is particularly intriguing considering that redox dyshomeostasis and the "unresponsive" gut phenotype have not been observed in other brain-first toxin-induced models of neurodegenerative diseases. This indicates that the damage induced by STZ-icv likely does not solely affect the GI tract by damaging the efferent control of gut function, such as via the efferent arm of the vagus nerve.

For instance, in the context of mimicking Parkinson's disease through intrastriatal administration of 6-hydroxydopamine, central neurodegeneration does not seem to lead to pronounced redox dyshomeostasis in the gut.[25] Although GI changes have been observed in this model,[83−85] they cannot be solely attributed to the absence of responsiveness to stimuli as a common factor.

Ultimately, gaining a more comprehensive understanding of the mechanisms contributing to the identified redox imbalance in the GI tract of the STZ-icv model could serve as a cornerstone for developing therapeutic strategies aimed at restoring redox balance and homeostasis in the STZ-icv gut. A pivotal aspect to delve into more thoroughly involves examining redox signaling and processes associated with lipid peroxidation that coincide with the observed alterations in the activity and expression of the antioxidant enzymes investigated

in this study. In this context, the scrutiny of 4-HNE, a prominent marker of lipid peroxidation and a crucial molecule in redox signaling,[86−89] may yield significant insights essential for a comprehensive understanding of the reported observations.

■ CONCLUSIONS

Together, the presented findings offer crucial insights into the mechanisms of redox dyshomeostasis in the gastrointestinal (GI) tract of the STZ-icv rat model of Alzheimer's disease (AD), as well as important information regarding the protective effects of D-galactose in the gut. In the STZ-induced gut dysfunction, there is a noticeable reduction in the ability of the redox regulatory system to maintain protection against free radicals, evidenced by the decreased activation of enzymes responsible for the immediate antioxidant defense and the upregulation of genes involved in the antioxidant response. The results obtained from control samples exposed to a prooxidative environment in the presence of D-galactose indicate that D-galactose can have beneficial effects on redox homeostasis. Specifically, it enhances antioxidant capacity, increases the activity of CAT and peroxidases, and stimulates the expression of SODs. However, these advantageous effects of D-galactose on redox homeostasis are less pronounced in the STZ-icv model of AD.

Limitations. The presented study has several important limitations that warrant consideration. First, although ex vivo experiments provide valuable insights into mechanisms by enabling precise control over experimental conditions, they may not entirely replicate the complex molecular events occurring in the actual *in vivo* environment. It is crucial to acknowledge this potential discrepancy when interpreting the results. Second, in this study, prooxidant conditions were simulated by subjecting duodenal rings to a single concentration of AAPH and H_2O_2, which aligns with established standards in the literature.[90,91] Moreover, to minimize bias introduced by decreased cell survival, the reaction was halted at a single time point (after 30 min of incubation). However, it is important to recognize that varying exposure times and concentrations of AAPH and H_2O_2 could lead to different outcomes and conclusions, and these alternative conditions should be considered in future investigations. Additionally, although we assessed cell survival in duodenal sections, we were unable to determine the spatial distribution of the expression of redox-related enzymes due to the limited availability of tissue samples. Consequently, we cannot pinpoint the specific cells driving the observed changes at the level of the whole tissue homogenate. While post-treatment microdissection was contemplated, the decreased survival of cells during the dissection process was associated with experimental error, leading us to dismiss this approach to avoid introducing bias. Therefore, it is essential to take these limitations into account when interpreting the study results and consider future research efforts to address these aspects comprehensively. Additionally, we wish to emphasize that, in the experiment conducted here, we employed H_2O_2 and AAPH incubation to mimic a "prooxidative environment" and assess compensatory cell responses. While the use of these two complementary conditions provided a broader understanding of the absence of response in the STZ samples, it is important to acknowledge that this approach was based on the assumption that these molecules would induce an oxidative environment without directly impacting the cells. In reality,

however, AAPH is a free-radical-generating azo compound capable of initiating oxidation through various complementary mechanisms. On the other hand, H_2O_2 is a stable, diffusible, nonradical oxidant that also plays roles in endogenous redox signaling.[4,73,92−94] H_2O_2 is a significant molecule involved in the regulation of redox and metabolic pathways through its interactions with multiple redox-sensitive proteins.[4,73,92−94] Consequently, its production and spatiotemporal patterns are tightly controlled within cells,[4,73,92−94] and it is probable that modeling the oxidative environment using H_2O_2 resulted in distinct effects on these pathways in both CTR and STZ samples. This is evident, for example, in the differential expression of CAT and the responses to prooxidative conditions. The differences in the response to H_2O_2 in the presence/absence of D-galactose also indicate alterations of the H_2O_2-associated pathways in the STZ samples. In this study, our primary emphasis was on investigating the expression and activity of antioxidant enzymes. We did not extensively examine lipid peroxidation,[95] a factor known to be crucial in pathophysiological processes associated with oxidative stress. The sole "redox biomarker" we employed concerning lipid peroxidation, TBARS, was assessed using a standard colorimetric method. It is important to note that this method has several analytical limitations, rendering it an unreliable tool for accurately assessing lipid peroxidation.[96−98] For this reason, the role of lipid peroxidation in the gastrointestinal tract of the STZ-icv model of AD and its involvement in the response to prooxidative condition in the presence or in the absence of D-galactose remain a topic of our future experiments. Preliminary findings from our prior experiments suggest a potential significance of lipid peroxidation. Despite the unreliability of TBARS as a marker for lipid peroxidation, measurements in our previous experiments indicate a potential increase in lipid peroxidation within the GI tract of the STZ-icv rat model of AD.[22] Moreover, oral administration of D-galactose appears to reduce TBARS in both the gastrointestinal tract and the brain.[64,65] However, a more in-depth analysis is required, utilizing more dependable biomarkers of lipid peroxidation, such as 4-HNE.[58,86,99] 4-HNE is of particular interest in this context, as it not only serves as a more reliable biomarker but also plays a crucial signaling role.[100] This aspect could be a key element in comprehending the hormetic effects of D-galactose.[64,65] In this study, the primary emphasis was on investigating the effects of D-galactose, given its known neuroprotective effects in the STZ-icv rat model of AD[28,61−63,76] and its positive impact on redox homeostasis in the GI tract.[64] Consequently, we opted not to include additional control conditions that would allow for the differentiation of the effects of galactose from those of structurally similar monosaccharides like glucose. While this choice was guided by scientific inquiry into the beneficial effects of supplementing the diet with low-dose galactose rather than substituting glucose with galactose, it is crucial to underscore that the presented results should be interpreted in consideration of the potential that some observed effects might not be specific to galactose. Future experiments incorporating additional control conditions are imperative to fully comprehend the role of D-galactose.

MATERIALS AND METHODS

Rat Model of Sporadic Alzheimer's Disease. The Croatian Ministry of Agriculture (EP 186/2018) and the Ethical Committee of the University of Zagreb School of Medicine (380−59−10106−18−111/173) approved all procedures. To establish the rat model of sAD, we utilized the intracerebroventricular administration of streptozotocin (STZ-icv) following a standard procedure[19,22,26,30] used and optimized in our laboratory since the original proposal of the model.[101] A total of eight 12-weeks-old male Wistar rats, bred under standardized conditions at the Department of Pharmacology, were randomly divided into two groups. The rats were anesthetized using intraperitoneal administration of ketamine/xylazine (70/7 mg/kg) and then subjected to intracerebroventricular treatment at specific coordinates relative to bregma (−1.5 mm posterior; ±1.5 mm lateral; +4 mm ventral).[102] Streptozotocin (STZ) was freshly dissolved in 0.05 M citrate buffer (pH 4.5), a standardly used vehicle.[26,30,35,41,101] Control animals (CTR; $n = 4$) were bilaterally injected with vehicle (2 μL/ventricle), and rats used for modeling sAD (STZ; $n = 4$) received STZ solution (2 μL/ventricle; 1.5 mg/kg). To attain an optimal response rate and minimize biological variability, the identical procedure was repeated 48 h later to accumulate a total dose of 3 mg/kg of STZ.[19,26,30] The most effective model induction protocol was established through our prior comprehensive research on the STZ-icv model.[19,26]

Tissue Harvesting for Ex Vivo Experiments. Duodenal rings for ex vivo experiments were obtained from 20-week-old animals (2 months after STZ-icv). The selection of this time frame is grounded in the following considerations: (i) it aligns with the "preclinical" phase of AD, as supported by existing research.[19,26,35,103] Intestinal homeostasis is recognized as a pivotal element in the development and initial stages of AD, underscoring the particular relevance of the early "preclinical" stage for comprehending functional alterations in the gastrointestinal tract; (ii) prior experiments have consistently shown that commencing oral D-galactose treatment during this preclinical stage of AD in the STZ-icv rat model can effectively prevent and improve cognitive impairments. When initiated at a later stage, oral D-galactose no longer confers neuroprotection.[28,61−64] Hence, this specific time point enabled us to assess the impact of D-galactose in a context that aids in the understanding of in vivo events; (iii) earlier studies have reported the presence of pathophysiological changes in the gastrointestinal tract during this time frame following STZ-icv administration.[22,24,41−43]

The animals were anesthetized (ip ketamine/xylazine; 70/7 mg/kg) and decapitated. Proximal duodenum was isolated and washed with preheated (35 °C) Krebs buffer (115 mM NaCl, 25 mM NaHCO$_3$, 2.4 mM K$_2$HPO$_4$, 1.2 mM CaCl$_2$, 1.2 mM MgCl$_2$, 0.4 mM KH$_2$PO$_4$, 10 mM glucose bubbled with carbogen gas (95% O$_2$; 5% CO$_2$) to remove intraluminal contents. Tissue was placed on top of a wet cellulose paper towel in a Petri dish filled with Krebs buffer and cut into 4 mm thick duodenal rings.

Treatments. Duodenal rings were incubated in a 96-well plate for 30 min. Control sections were incubated in Krebs buffer (CTR); pro-oxidative environment was modeled by incubation with 200 μM 2,2′-Azobis(2-amidinopropane) dihydrochloride in Krebs buffer (AAPH) or 1.5 mM H$_2$O$_2$ in Krebs buffer (H$_2$O$_2$). The ability of D-galactose to protect the tissue against oxidative challenge was investigated by incubation with 100 mM D-galactose in the presence of 200 μM AAPH (AAPH + GAL) or 1.5 mM H$_2$O$_2$ (H$_2$O$_2$ + GAL). The chosen concentration of D-galactose was based on its observed beneficial effects in the GI tract when administered

acutely at a cumulative daily dose of 200 mg/kg (dissolved in 1 mL of water), as demonstrated in previous research.[64] This concentration also exhibited neuroprotective effects when it was administered continuously by dissolving it in water and providing unrestricted access.[28,63] In the acute treatment scenario, where positive impacts on redox homeostasis have been noted, the D-galactose concentration in the 1 mL solution given via oral gavage equated to approximately 550 mM.[64] Considering the fluid volume in the rat's stomach and upper small intestine, the administered solution's concentration is expected to be diluted roughly 5-fold after administration, leading to an exposure of the duodenal mucosa to approximately 100 mM D-galactose. An approximate comparison of duodenal exposure to D-galactose in humans could be achieved by consuming 200 mL of cow's milk, assuming the following conditions: (i) D-galactose was completely released from lactose (e.g., lactase-based lactose-free milk); (ii) the remaining gastric fluid volume in humans ranges from 20 to 100 mL (averaging 60 mL); and (iii) 200 mL of cow's milk typically contains an average of 10 g of lactose, equivalent to 5 g of D-galactose.

Tissue Preparation. Duodenal rings were removed from the experimental solution, rinsed in Krebs buffer, snap-frozen in liquid nitrogen, and stored at -80 °C. Samples were homogenized with ultrasonic waves (Microson Ultrasonic Cell 167 Disruptor XL, Misonix, Farmingdale, NY, SAD) in lysis buffer containing 150 mM NaCl, 50 mM Tris-HCl, 1 mM EDTA, 1% Triton X-100, 1% sodium deoxycholate, 0.1% SDS, 1 mM PMSF, protease (Sigma-Aldrich, Burlington, MA, USA) and phosphatase inhibitor (PhosSTOP, Roche, Basel, Switzerland) cocktail (pH 7.5). Homogenates were centrifuged (relative centrifugal force (RCF) 12,879g) for 10 min at 4 °C. Protein concentration in supernatants was analyzed with the Bradford reagent (Sigma-Aldrich, USA) using bovine serum albumin in lysis buffer as a standard solution. Samples were stored at -80 °C.

DAPI Permeability Assay. DAPI permeability assays was performed to label dead cells for subsequent analysis. A set of duodenal rings adjacent to the rings used for the analysis of redox biomarkers and subjected to the same treatment (CTR, AAPH, H_2O_2, AAPH + GAL, H_2O_2 + GAL) was rinsed in Krebs buffer and immersed for 5 min in Krebs buffer containing 4′,6-diamidino-2-phenylindole (DAPI; 1 μg/mL). After incubation, samples were rinsed in Krebs buffer and stored in 4% paraformaldehyde (pH 7.4) at 4 °C. Tissue sections were cut using a cryostat (Leica, Germany) following fixation in Tissue-Tek O.C.T (Akura Finetek USA, USA). Samples were coverslipped with Fluoroshield mounting medium (9 parts glycerol, 1 part 10× PBS, 2% n-propyl gallate) and analyzed using the U-MNU2 filter set (EX: 365/10; EM: >420) on the Olympus BX51 epifluorescent microscope (Olympus, Japan). Images were analyzed in Fiji (NIH, USA).

Analysis of Redox Biomarkers. Total antioxidant capacity was analyzed with 2,2′-azino-bis(3-ethylbenzothiazoline-6-sulfonic acid)(ABTS) radical cation assay[104] and NRP.[66] Briefly, the ABTS radical cation was generated by reacting 7 mM ABTS with 2.45 mM $K_2S_2O_8$ in the dark for 24 h. The solution was diluted 40-fold in PBS to obtain optimal baseline absorbance. Tissue homogenates (1 μL) were incubated with 100 μL of the ABTS working solution in 96-well plates and 405 nm absorbance was recorded after 5 min using an Infinite F200 PRO multimodal microplate reader (Tecan, Switzer-

land). 1,4-dithiothreitol (DTT) was used as a standard reducing agent.[105] NRP was measured by first spotting 1 μL of each sample on the nitrocellulose membrane (Amersham Protran 0.45; GE Healthcare Life Sciences, USA). A dry membrane was immersed in NRP working solution (10 mg/mL KMnO$_4$ in ddH$_2$O). The membrane was destained in dH$_2$O, dried, scanned, and analyzed in Fiji with a Gel Analyzer plugin, as described previously.[66] Activity of SODs was determined with a modified 1,2,3-trihydroxybenzene (THB) autoxidation inhibition assay.[106−108] Reaction buffer contained 0.05 M Tris-HCl and 1 mM Na$_2$EDTA (pH 8.2), and the final concentration of THB was 1.2 mM. Reaction buffer was modified by adding 2 mM KCN to discriminate between Cu/Zn- and Mn/Fe-SOD.[25] THB autoxidation was monitored at 450 nm with a multimodal microplate reader (Tecan, Switzerland). Catalase and peroxidase activities were determined indirectly by quantifying residual H_2O_2 assessed by Co oxidation after incubation with 10 mM H_2O_2 in PBS.[109] Samples (10 μL) were first incubated with 40 μL of 10 mM H_2O_2 for 90 s and then reacted with 100 μL of Co(NO$_3$)$_2$ working solution. Baseline interference was ruled out by reacting the samples with stop solution before adding the substrate.[25,110] Carbonato-cobaltate (III) complex ([Co-(CO$_3$)$_3$]Co) absorbance was measured at 450 nm with a microplate reader (Tecan, Switzerland) and compared to the H_2O_2 standard model to determine the H_2O_2 concentration. The same procedure was repeated in the presence of 25 μM NaN$_3$ to discriminate between the activity of catalase and peroxidases.[25,111] Reaction conditions were optimzied in pilot experiments. Lipid peroxidation was assessed with the thiobarbituric acid reactive substances (TBARS) assay.[65] Tissue homogenates (20 μL) were mixed with the TBA-TCA solution [0.4% thiobarbituric acid (Kemika, Croatia); 15% trichloroacetic acid (Sigma-Aldrich, USA)] in perforated microcentrifuge tubes. The samples were boiled at 95 °C for 45 min, and the colored adduct was extracted with n-butanol. The absorbance of butanol extracts was measured at 540 nm in a 384-well plate by using the Infinite F200 PRO multimodal plate reader (Tecan, Switzerland). Malondialdehyde tetrabutylammonium in ddH$_2$O (Sigma-Aldrich, USA) serial dilutions was processed in parallel to obtain a standard curve. Reaction steps were optimized in pilot experiments.

Protein Microarray. Expression of proteins of interest [catalase (CAT), superoxide dismutase 1 (SOD1), superoxide dismutase 2 (SOD2), glutathione peroxidase 4 (GPX4), and neuronal nitric oxide synthase (nNOS)] was analyzed with an indirect immunofluorescence-based microarray. Samples were fixed onto a nitrocellulose membrane by using a PVC template. Fixed samples were blocked in a blocking buffer [10 mM Tris, 150 mM NaCl, 5% (w/v) nonfat dry milk, 0,5% (v/v) Tween 20 (pH 7.5)] at room temperature for 1 h. Membranes were incubated with primary antibodies diluted in the blocking buffer [anti-CAT (ABIN872991; 1:400), anti-SOD1-(ABIN2854826; 1:400), anti-SOD2 (PA1776; 1:400), anti-GPX4 (CQA1094; 1:400), anti-nNOS (PA1329; 1:400)] for 24 h at +4 °C. Membranes were washed in 1× PBS and incubated with antirabbit IgG (H + L) F(ab′)$_2$ fragment conjugated to Alexa Fluor 488 (4412S; 1:500; Cell Signaling Technology, USA) for 2 h at room temperature. Unbound antibodies were removed in 1× PBS, and sample fluorescence was recorded using ChemiDoc MP Imaging System (Bio-Rad, USA)(EX/EM (nm): 460−490/518−546). Background fluorescence was recorded (EX/EM (nm): 302/535−645) for

adjustment. Protein expression data were obtained using a pipeline, in which the expression was determined based on 460−490/518−546 fluorescence adjusted for autofluorescence (302/535−645) and protein concentration.

Quantification of Nitrites. The Griess assay was utilized to indirectly quantify nitric oxide (NO) by measuring the nitrite concentration. The modified Griess reagent (Sigma-Aldrich, USA), consisting of naphthylethylenediamine dihydrochloride and sulphanilamide in phosphoric acid, was employed in the assay. To accommodate the 384-well plate format, optimal sample volumes were adjusted and mixed in a 1:1 volumetric ratio with the Griess working solution [0.4% (w/v)]. The absorbance change was measured at 540 nm over a period of 15 min.

Data Analysis. Data analysis was conducted using R (4.1.3) adhering to the guidelines for reporting animal experiments.[112] The statistical modeling approach employed linear-mixed models to address the hierarchical structure of the data. In this approach, redox biomarkers were designated as the dependent variables, while the independent variables included group (CTR vs STZ), treatment (CTR, AAPH, H_2O_2, AAPH + GAL, H_2O_2 + GAL), and the interaction between group and treatment. Moreover, the protein concentration was included as a covariate to address any potential bias that may have arisen during sample preparation procedures. Additional covariates were also introduced when necessary, such as baseline H_2O_2 in the CAT model, to further control for relevant factors. Sample nonspecific fluorescence was introduced as an additional covariate in protein expression models. The animal identification number was defined as a random effect to account for the hierarchical structure. Model assumptions were verified through visual inspection of residual and fitted value plots, and if required, variable transformations were applied. Model estimates were presented as effect sizes, along with their corresponding 95% confidence intervals. The results were presented in two ways: (i) as contrasts of groups (CTR vs STZ) at the levels of treatments (CTR/AAPH/H_2O_2/AAPH+GAL/H_2O_2+GAL) and (ii) as contrasts of the control and experimental conditions (CTR vs AAPH/H_2O_2/AAPH+GAL/H_2O_2+GAL) for CTR and STZ groups individually. H_2O_2 and SOD signaling pathways were modeled with structural equation modeling (SEM) in *lavaan*.[113] Enzyme expression and activity data were utilized as manifest variables to create latent variables for H_2O_2 and SOD signaling. In the H_2O_2 model, the covariance between CAT expression and baseline H_2O_2, as well as the covariance between total H_2O_2 dissociation capacity and baseline H_2O_2, were both included. Similarly, in the SOD model, the covariance between SOD1 and SOD2 expression and the covariance between SOD2 expression and SOD2 activity were incorporated based on modification indices. To assess the suitability of SEMs, goodness-of-fit indices such as Comparative Fit Index (CFI) and Tucker−Lewis Index (TLI) and badness-of-fit indices including root mean square error of approximation (RMSEA) and standardized root mean square residual (SRMSR) were evaluated. Standardized loadings were reported to assess the relationships between latent and manifest variables. Differences of H_2O_2 and SOD pathways between groups (CTR vs STZ) were analyzed with a χ^2 difference test. α was fixed at 5%. Nonlinear dimensionality reduction was performed using a uniform manifold approximation and projection (UMAP). Both SEM and UMAP analyses were performed on scaled data sets.

■ ASSOCIATED CONTENT

Data Availability Statement
Raw data for the study can be obtained from the corresponding author upon request. Preprinted on bioRxiv (DOI: 10.1101/2023.07.27.550831).

■ AUTHOR INFORMATION

Corresponding Author
Jan Homolak − *Department of Pharmacology & Croatian Institute for Brain Research, University of Zagreb School of Medicine, 10000 Zagreb, Croatia; Interfaculty Institute of Microbiology and Infection Medicine Tübingen, University of Tübingen, 72074 Tübingen, Germany;* ⬤ orcid.org/0000-0003-1508-3243; Phone: +385 91 9411468; Email: homolakjan@gmail.com, jan.homolak@mef.hr, Jan.Homolak@med.uni-tuebingen.de

Authors
Konstantinos Varvaras − *Department of Medicine, School of Health Sciences, Aristotle University of Thessaloniki, 54124 Thessaloniki, Greece;* ⬤ orcid.org/0009-0007-1060-8561

Vittorio Sciacca − *Faculty of Medicine, University of Catania, 95131 Catania, Italy*

Ana Babic Perhoc − *Department of Pharmacology & Croatian Institute for Brain Research, University of Zagreb School of Medicine, 10000 Zagreb, Croatia*

Davor Virag − *Department of Pharmacology & Croatian Institute for Brain Research, University of Zagreb School of Medicine, 10000 Zagreb, Croatia*

Ana Knezovic − *Department of Pharmacology & Croatian Institute for Brain Research, University of Zagreb School of Medicine, 10000 Zagreb, Croatia*

Jelena Osmanovic Barilar − *Department of Pharmacology & Croatian Institute for Brain Research, University of Zagreb School of Medicine, 10000 Zagreb, Croatia*

Melita Salkovic-Petrisic − *Department of Pharmacology & Croatian Institute for Brain Research, University of Zagreb School of Medicine, 10000 Zagreb, Croatia*

Complete contact information is available at:
https://pubs.acs.org/10.1021/acsomega.3c07152

Author Contributions
J.H.: Study design; A.B.P., A.K., D.V., J.O.B., and J.H.: model induction and behavioral assessment; J.H.: ex vivo experiment; K.V., V.S., and J.H.: biochemical analyses; K.V. and V.S.: tissue processing and image acquisition; J.H. and K.V.: data curation; J.H.: data analysis and writing the first draft of the manuscript; K.V., V.S., A.B.P., A.K., D.V., J.O.B., and M.S.P.: critical revision of the manuscript; M.S.P.: funding and supervision.

Notes
The animal procedures were conducted following the guidelines of the University of Zagreb School of Medicine, as well as

the national regulations outlined in The Animal Protection Act (NN135/2006; NN 47/2011) and international guidelines from Directive 2010/63/EU on the use of experimental animals. Approval for the experiments was obtained from both the Croatian Ministry of Agriculture (EP 186/2018; 525−10/0255−15−5) and the Ethical Committee of the University of Zagreb School of Medicine (380−59−10106−18−111/173). The authors declare no competing financial interest.

■ REFERENCES

(1) Singh, A.; Dawson, T. M.; Kulkarni, S. Neurodegenerative disorders and gut-brain interactions. *J. Clin Invest.* **2021**, *131*, No. e143775.

(2) Bhattacharyya, A.; Chattopadhyay, R.; Mitra, S.; Crowe, S. E. Oxidative stress: an essential factor in the pathogenesis of gastrointestinal mucosal diseases. *Physiol Rev.* **2014**, *94*, 329−354.

(3) Bischoff, S. C.; Barbara, G.; Buurman, W.; Ockhuizen, T.; Schulzke, J.-D.; Serino, M.; Tilg, H.; Watson, A.; Wells, J. M. Intestinal permeability–a new target for disease prevention and therapy. *BMC Gastroenterol.* **2014**, *14*, 189.

(4) Homolak, J. Gastrointestinal redox homeostasis in ageing. *Biogerontology.* **2023**, *24*, 741.

(5) Homolak, J. Targeting the microbiota-mitochondria crosstalk in neurodegeneration with senotherapeutics. *Adv. Protein Chem. Struct Biol.* **2023**, *136*, 339−383.

(6) Chassaing, B.; Kumar, M.; Baker, M. T.; Singh, V.; Vijay-Kumar, M. Mammalian gut immunity. *Biomed J.* **2014**, *37*, 246−258.

(7) Alves, S. S.; da Silva-Junior, R. M. P.; Servilha-Menezes, G.; Homolak, J.; Šalković-Petrišić, M.; Garcia-Cairasco, N. Insulin Resistance as a Common Link Between Current Alzheimer's Disease Hypotheses. *J. Alzheimers Dis.* **2021**, *82*, 71−105.

(8) Homolak, J., Redox Homeostasis in Alzheimer's Disease, in: Çakatay, U. (Ed.), *Redox Signaling and Biomarkers in Ageing*; Springer International Publishing: Cham, 2022: 323−348.

(9) Barnham, K. J.; Masters, C. L.; Bush, A. I. Neurodegenerative diseases and oxidative stress. *Nat. Rev. Drug Discovery* **2004**, *3*, 205−214.

(10) Perry, V. H.; Cunningham, C.; Holmes, C. Systemic infections and inflammation affect chronic neurodegeneration. *Nat. Rev. Immunol.* **2007**, *7*, 161−167.

(11) Brown, G. C. The endotoxin hypothesis of neurodegeneration. *J. Neuroinflammation.* **2019**, *16*, 180.

(12) Qian, X.-H.; Song, X.-X.; Liu, X.-L.; Chen, S.; Tang, H.-D. Inflammatory pathways in Alzheimer's disease mediated by gut microbiota. *Ageing Res. Rev.* **2021**, *68*, No. 101317.

(13) Carabotti, M.; Scirocco, A.; Maselli, M. A.; Severi, C. The gut-brain axis: interactions between enteric microbiota, central and enteric nervous systems. *Ann. Gastroenterol.* **2015**, *28*, 203−209. https://www.ncbi.nlm.nih.gov/pmc/articles/PMC4367209/ (accessed April 1, 2023).

(14) Herath, M.; Hosie, S.; Bornstein, J. C.; Franks, A. E.; Hill-Yardin, E. L. The Role of the Gastrointestinal Mucus System in Intestinal Homeostasis: Implications for Neurological Disorders. *Front Cell Infect Microbiol.* **2020**, *10*, 248.

(15) Honarpisheh, P.; Reynolds, C. R.; Blasco Conesa, M. P.; Moruno Manchon, J. F.; Putluri, N.; Bhattacharjee, M. B.; Urayama, A.; McCullough, L. D.; Ganesh, B. P. Dysregulated Gut Homeostasis Observed Prior to the Accumulation of the Brain Amyloid-β in Tg2576 Mice. *Int. J. Mol. Sci.* **2020**, *21*, 1711.

(16) Semar, S.; Klotz, M.; Letiembre, M.; Van Ginneken, C.; Braun, A.; Jost, V.; Bischof, M.; Lammers, W. J.; Liu, Y.; Fassbender, K.; Wyss-Coray, T.; Kirchhoff, F.; Schäfer, K.-H. Changes of the enteric nervous system in amyloid-β protein precursor transgenic mice correlate with disease progression. *J. Alzheimers Dis.* **2013**, *36*, 7−20.

(17) Homolak, J.; Babic Perhoc, A.; Knezovic, A.; Osmanovic Barilar, J.; Virag, D.; Salkovic-Petrisic, M. Exploratory Study of Gastrointestinal Redox Biomarkers in the Presymptomatic and Symptomatic Tg2576 Mouse Model of Familial Alzheimer's Disease:

Phenotypic Correlates and Effects of Chronic Oral d-Galactose. *ACS Chem. Neurosci.* **2023**, *14*, 4013−4025.

(18) Sajadi, A.; Provost, C.; Pham, B.; Brouillette, J. Neurodegeneration in an Animal Model of Chronic Amyloid-beta Oligomer Infusion Is Counteracted by Antibody Treatment Infused with Osmotic Pumps. *J. Vis Exp.* **2016**, 54215.

(19) M., Salkovic-Petrisic; Perhoc, A.B.; Homolak, J.; Knezovic, A.; J., Osmanovic Barilar; Riederer, P. Experimental Approach to Alzheimer's Disease with Emphasis on Insulin Resistance in the Brain, in: Kostrzewa, R.M. (Ed.), *Handbook of Neurotoxicity*; Springer International Publishing: Cham, 2021: 1−52.

(20) Raghavendra, M.; Maiti, R.; Kumar, S.; Acharya, S. Role of aqueous extract of Azadirachta indica leaves in an experimental model of Alzheimer's disease in rats. *Int. J. Appl. Basic Med. Res.* **2013**, *3*, 37−47.

(21) Broetto, N.; Hansen, F.; Brolese, G.; Batassini, C.; Lirio, F.; Galland, F.; Dos Santos, J. P. A.; Dutra, M. F.; Gonçalves, C.-A. Intracerebroventricular administration of okadaic acid induces hippocampal glucose uptake dysfunction and tau phosphorylation. *Brain Res. Bull.* **2016**, *124*, 136−143.

(22) Homolak, J.; Babic Perhoc, A.; Knezovic, A.; Osmanovic Barilar, J.; Salkovic-Petrisic, M. Failure of the Brain Glucagon-Like Peptide-1-Mediated Control of Intestinal Redox Homeostasis in a Rat Model of Sporadic Alzheimer's Disease. *Antioxidants (Basel).* **2021**, *10*, 1118.

(23) Homolak, J., *Pathophysiological alterations of gastrointestinal system in animal models of Alzheimer's and Parkinson's disease*, info:eu-repo/semantics/doctoralThesis; University of Zagreb. School of Medicine, 2023. https://urn.nsk.hr/urn:nbn:hr:105:754088 (accessed July 1, 2023).

(24) Homolak, J.; De Busscher, J.; Zambrano-Lucio, M.; Joja, M.; Virag, D.; Babic Perhoc, A.; Knezovic, A.; Osmanovic Barilar, J.; Salkovic-Petrisic, M. Altered Secretion, Constitution, and Functional Properties of the Gastrointestinal Mucus in a Rat Model of Sporadic Alzheimer's Disease. *ACS Chem. Neurosci.* **2023**, *14*, 2667.

(25) Homolak, J.; Joja, M.; Grabaric, G.; Schiatti, E.; Virag, D.; Perhoc, A.B.; Knezovic, A.; Barilar, J.O.; Salkovic-Petrisic, M. The absence of gastrointestinal redox dyshomeostasis in the brain-first rat model of Parkinson's disease induced by bilateral intrastriatal 6-hydroxydopamine. *Mol. Neurobiol.* **2024**, DOI: 10.1007/s12035-023-03906-7.

(26) Homolak, J.; Perhoc, A.B.; Knezovic, A.; J., Osmanovic Barilar; M., Salkovic-Petrisic Additional methodological considerations regarding optimization of the dose of intracerebroventricular streptozotocin A response to: "Optimization of intracerebroventricular streptozotocin dose for the induction of neuroinflammation and memory impairments in rats by Ghosh et al., Metab Brain Dis **2021** July 21, *Metab Brain Dis. 36* (2021) 97−102, DOI: .

(27) Correia, S. C.; Santos, R. X.; Perry, G.; Zhu, X.; Moreira, P. I.; Smith, M. A. Insulin-Resistant Brain State: the culprit in sporadic Alzheimer's Disease? *Ageing Res. Rev.* **2011**, *10*, 264−273.

(28) Knezovic, A.; Osmanovic Barilar, J.; Babic, A.; Bagaric, R.; Farkas, V.; Riederer, P.; Salkovic-Petrisic, M. Glucagon-like peptide-1 mediates effects of oral galactose in streptozotocin-induced rat model of sporadic Alzheimer's disease. *Neuropharmacology.* **2018**, *135*, 48−62.

(29) Sharma, M.; Gupta, Y. K. Intracerebroventricular injection of streptozotocin in rats produces both oxidative stress in the brain and cognitive impairment. *Life Sci.* **2001**, *68*, 1021−1029.

(30) Knezovic, A.; Loncar, A.; Homolak, J.; Smailovic, U.; Osmanovic Barilar, J.; Ganoci, L.; Bozina, N.; Riederer, P.; Salkovic-Petrisic, M. Rat brain glucose transporter-2, insulin receptor and glial expression are acute targets of intracerebroventricular streptozotocin: risk factors for sporadic Alzheimer's disease? *J. Neural Transm (Vienna).* **2017**, *124*, 695−708.

(31) Ghosh, R.; Sil, S.; Gupta, P.; Ghosh, T. Optimization of intracerebroventricular streptozotocin dose for the induction of neuroinflammation and memory impairments in rats. *Metab Brain Dis.* **2020**, *35*, 1279−1286.

(32) Li, Y.; Xu, P.; Shan, J.; Sun, W.; Ji, X.; Chi, T.; Liu, P.; Zou, L. Interaction between hyperphosphorylated tau and pyroptosis in forskolin and streptozotocin induced AD models. *Biomed Pharmacother.* **2020**, *121*, No. 109618.

(33) Salkovic-Petrisic, M.; Osmanovic-Barilar, J.; Brückner, M. K.; Hoyer, S.; Arendt, T.; Riederer, P. Cerebral amyloid angiopathy in streptozotocin rat model of sporadic Alzheimer's disease: a long-term follow up study. *J. Neural Transm (Vienna).* **2011**, *118*, 765−772.

(34) Grünblatt, E.; Homolak, J.; Babic Perhoc, A.; Davor, V.; Knezovic, A.; Osmanovic Barilar, J.; Riederer, P.; Walitza, S.; Tackenberg, C.; Salkovic-Petrisic, M. From attention-deficit hyperactivity disorder to sporadic Alzheimer's disease-Wnt/mTOR pathways hypothesis. *Front Neurosci.* **2023**, *17*, No. 1104985.

(35) Knezovic, A.; Osmanovic-Barilar, J.; Curlin, M.; Hof, P. R.; Simic, G.; Riederer, P.; Salkovic-Petrisic, M. Staging of cognitive deficits and neuropathological and ultrastructural changes in streptozotocin-induced rat model of Alzheimer's disease. *J. Neural Transm (Vienna).* **2015**, *122*, 577−592.

(36) Hosokawa, M.; Dolci, W.; Thorens, B. Differential sensitivity of GLUT1- and GLUT2-expressing beta cells to streptozotocin. *Biochem. Biophys. Res. Commun.* **2001**, *289*, 1114−1117.

(37) Yamamoto, H.; Uchigata, Y.; Okamoto, H. Streptozotocin and alloxan induce DNA strand breaks and poly(ADP-ribose) synthetase in pancreatic islets. *Nature.* **1981**, *294*, 284−286.

(38) Nahdi, A. M. T. A.; John, A.; Raza, H. Elucidation of Molecular Mechanisms of Streptozotocin-Induced Oxidative Stress, Apoptosis, and Mitochondrial Dysfunction in Rin-5F Pancreatic β-Cells. *Oxid. Med. Cell Longev.* **2017**, *2017*, No. 7054272.

(39) Van Dyke, K.; Ghareeb, E.; Van Dyke, M.; Sosa, A.; Hoeldtke, R. D.; Van Thiel, D. H. Luminescence experiments involved in the mechanism of streptozotocin diabetes and cataract formation. *Luminescence.* **2008**, *23*, 386−391.

(40) Grieb, P. Intracerebroventricular Streptozotocin Injections as a Model of Alzheimer's Disease: in Search of a Relevant Mechanism. *Mol. Neurobiol.* **2016**, *53*, 1741−1752.

(41) Homolak, J.; Babic Perhoc, A.; Knezovic, A.; Osmanovic Barilar, J.; Koc, F.; Stanton, C.; Ross, R. P.; Salkovic-Petrisic, M. Disbalance of the Duodenal Epithelial Cell Turnover and Apoptosis Accompanies Insensitivity of Intestinal Redox Homeostasis to Inhibition of the Brain Glucose-Dependent Insulinotropic Polypeptide Receptors in a Rat Model of Sporadic Alzheimer's Disease. *Neuroendocrinology.* **2022**, *112*, 744−762.

(42) Osmanović Barilar, J.; Babić Perhoč, A.; Knezović, A.; Homolak, J.; Virag, D.; Šalković-Petrišić, M. The Effect of the Sodium-Glucose Cotransporter Inhibitor on Cognition and Metabolic Parameters in a Rat Model of Sporadic Alzheimer's Disease. *Biomedicines.* **2023**, *11*, 1025.

(43) Moraes, R. C. M. d.; Lima, G. C. A.; Cardinali, C. A. E. F.; Gonçalves, A. C.; Portari, G. V.; Guerra-Shinohara, E. M.; Leboucher, A.; Donato, J.; Kleinridders, A.; Torrão, A. d. S. Benfotiamine protects against hypothalamic dysfunction in a STZ-induced model of neurodegeneration in rats. *Life Sci.* **2022**, *306*, No. 120841.

(44) Singh, A.; Kukreti, R.; Saso, L.; Kukreti, S. Oxidative Stress: A Key Modulator in Neurodegenerative Diseases. *Molecules.* **2019**, *24*, 1583.

(45) Kim, G. H.; Kim, J. E.; Rhie, S. J.; Yoon, S. The Role of Oxidative Stress in Neurodegenerative Diseases. *Exp Neurobiol.* **2015**, *24*, 325−340.

(46) Uttara, B.; Singh, A. V.; Zamboni, P.; Mahajan, R. T. Oxidative Stress and Neurodegenerative Diseases: A Review of Upstream and Downstream Antioxidant Therapeutic Options. *Curr. Neuropharmacol.* **2009**, *7*, 65−74.

(47) Butterfield, D. A.; Halliwell, B. Oxidative stress, dysfunctional glucose metabolism and Alzheimer disease. *Nat. Rev. Neurosci.* **2019**, *20*, 148−160.

(48) Marcus, D. L.; Thomas, C.; Rodriguez, C.; Simberkoff, K.; Tsai, J. S.; Strafaci, J. A.; Freedman, M. L. Increased Peroxidation and Reduced Antioxidant Enzyme Activity in Alzheimer's Disease. *Exp. Neurol.* **1998**, *150*, 40−44.

(49) Pamplona, R.; Dalfó, E.; Ayala, V.; Bellmunt, M. J.; Prat, J.; Ferrer, I.; Portero-Otín, M. Proteins in Human Brain Cortex Are Modified by Oxidation, Glycoxidation, and Lipoxidation: EFFECTS OF ALZHEIMER DISEASE AND IDENTIFICATION OF LIP-OXIDATION TARGETS*. *J. Biol. Chem.* **2005**, *280*, 21522−21530.

(50) Arslan, J.; Jamshed, H.; Qureshi, H. Early Detection and Prevention of Alzheimer's Disease: Role of Oxidative Markers and Natural Antioxidants. *Front. Aging Neurosci.* **2020**, *12*, 231 DOI: 10.3389/fnagi.2020.00231. https://www.frontiersin.org/articles/10.3389/fnagi.2020.00231 (accessed November 11, 2023)

(51) Wang, X.; Wang, W.; Li, L.; Perry, G.; Lee, H.; Zhu, X. Oxidative stress and mitochondrial dysfunction in Alzheimer's disease. *Biochimica et Biophysica Acta (BBA) - Molecular Basis of Disease.* **2014**, *1842*, 1240−1247.

(52) Ionescu-Tucker, A.; Cotman, C. W. Emerging roles of oxidative stress in brain aging and Alzheimer's disease. *Neurobiology of Aging.* **2021**, *107*, 86−95.

(53) Chen, Z.; Zhong, C. Oxidative stress in Alzheimer's disease. *Neurosci Bull.* **2014**, *30*, 271−281.

(54) Forman, H. J.; Zhang, H. Targeting oxidative stress in disease: promise and limitations of antioxidant therapy. *Nat. Rev. Drug Discovery* **2021**, *20*, 689−709.

(55) Kamat, P. K.; Kalani, A.; Rai, S.; Swarnkar, S.; Tota, S.; Nath, C.; Tyagi, N. Mechanism of Oxidative Stress and Synapse Dysfunction in the Pathogenesis of Alzheimer's Disease: Understanding the Therapeutics Strategies. *Mol. Neurobiol.* **2016**, *53*, 648−661.

(56) Bai, R.; Guo, J.; Ye, X.-Y.; Xie, Y.; Xie, T. Oxidative stress: The core pathogenesis and mechanism of Alzheimer's disease. *Ageing Research Reviews.* **2022**, *77*, No. 101619.

(57) Smith, M. A.; Rottkamp, C. A.; Nunomura, A.; Raina, A. K.; Perry, G. Oxidative stress in Alzheimer's disease. *Biochimica et Biophysica Acta (BBA) - Molecular Basis of Disease.* **2000**, *1502*, 139−144.

(58) Zarkovic, K. 4-hydroxynonenal and neurodegenerative diseases. *Mol. Aspects Med.* **2003**, *24*, 293−303.

(59) Vaccaro, A.; Kaplan Dor, Y.; Nambara, K.; Pollina, E. A.; Lin, C.; Greenberg, M. E.; Rogulja, D. Sleep Loss Can Cause Death through Accumulation of Reactive Oxygen Species in the Gut. *Cell* **2020**, *181*, 1307−1328.e15.

(60) Sadigh-Eteghad, S.; Majdi, A.; McCann, S. K.; Mahmoudi, J.; Vafaee, M. S.; Macleod, M. R. D-galactose-induced brain ageing model: A systematic review and meta-analysis on cognitive outcomes and oxidative stress indices. *PLoS One.* **2017**, *12*, No. e0184122.

(61) Babic Perhoc, A.; Osmanovic Barilar, J.; Knezovic, A.; Farkas, V.; Bagaric, R.; Svarc, A.; Grünblatt, E.; Riederer, P.; Salkovic-Petrisic, M. Cognitive, behavioral and metabolic effects of oral galactose treatment in the transgenic Tg2576 mice. *Neuropharmacology.* **2019**, *148*, 50−67.

(62) Salkovic-Petrisic, M. Oral Galactose Provides a Different Approach to Incretin-Based Therapy of Alzheimer's Disease. *J. Neurol. Neuromed.* **2018**, *3* (4), 101−107, DOI: 10.29245/2572.942X/2018/4.1204. https://www.jneurology.com/articles/oral-galactose-provides-a-different-approach-to-incretinbased-therapy-of-alzheimers-disease.html (accessed March 25, 2023).

(63) Salkovic-Petrisic, M.; Osmanovic-Barilar, J.; Knezovic, A.; Hoyer, S.; Mosetter, K.; Reutter, W. Long-term oral galactose treatment prevents cognitive deficits in male Wistar rats treated intracerebroventricularly with streptozotocin. *Neuropharmacology.* **2014**, *77*, 68−80.

(64) Homolak, J.; Babic Perhoc, A.; Knezovic, A.; Osmanovic Barilar, J.; Virag, D.; Joja, M.; Salkovic-Petrisic, M. The Effect of Acute Oral Galactose Administration on the Redox System of the Rat Small Intestine. *Antioxidants (Basel).* **2022**, *11*, 37.

(65) Homolak, J.; Babic Perhoc, A.; Knezovic, A.; Kodvanj, I.; Virag, D.; Osmanovic Barilar, J.; Riederer, P.; Salkovic-Petrisic, M. Is Galactose a Hormetic Sugar? An Exploratory Study of the Rat Hippocampal Redox Regulatory Network. *Mol. Nutr Food Res.* **2021**, *65*, No. e2100400.

(66) Homolak, J.; Kodvanj, I.; Babic Perhoc, A.; Virag, D.; Knezovic, A.; Osmanovic Barilar, J.; Riederer, P.; Salkovic-Petrisic, M. Nitrocellulose redox permanganometry: A simple method for reductive capacity assessment. *MethodsX.* 2022, 9, No. 101611.

(67) Yano, S.; Yano, N. Regulation of catalase enzyme activity by cell signaling molecules. *Mol. Cell. Biochem.* 2002, 240, 119−130.

(68) Tsang, C. K.; Chen, M.; Cheng, X.; Qi, Y.; Chen, Y.; Das, I.; Li, X.; Vallat, B.; Fu, L.-W.; Qian, C.-N.; Wang, H.-Y.; White, E.; Burley, S. K.; Zheng, X. F. S. SOD1 Phosphorylation by mTORC1 Couples Nutrient Sensing and Redox Regulation. *Mol. Cell* 2018, 70, 502−515.e8.

(69) Vomhof-Dekrey, E. E.; Picklo, M. J. The Nrf2-antioxidant response element pathway: a target for regulating energy metabolism. *J. Nutr Biochem.* 2012, 23, 1201−1206.

(70) Nguyen, T.; Nioi, P.; Pickett, C. B. The Nrf2-antioxidant response element signaling pathway and its activation by oxidative stress. *J. Biol. Chem.* 2009, 284, 13291−13295.

(71) Li, W.; Kong, A.-N. Molecular mechanisms of Nrf2-mediated antioxidant response. *Mol. Carcinog.* 2009, 48, 91−104.

(72) Milkovic, L.; Zarkovic, N.; Saso, L. Controversy about pharmacological modulation of Nrf2 for cancer therapy. *Redox Biol.* 2017, 12, 727−732.

(73) Atayik, M. C.; Çakatay, U. Redox signaling and modulation in ageing. *Biogerontology.* 2023, 24, 603−608.

(74) Hwang, J.; Jin, J.; Jeon, S.; Moon, S. H.; Park, M. Y.; Yum, D.-Y.; Kim, J. H.; Kang, J.-E.; Park, M. H.; Kim, E.-J.; Pan, J.-G.; Kwon, O.; Oh, G. T. SOD1 suppresses pro-inflammatory immune responses by protecting against oxidative stress in colitis. *Redox Biol.* 2020, 37, No. 101760.

(75) Zhu, T.; Wang, Z.; He, J.; Zhang, X.; Zhu, C.; Zhang, S.; Li, Y.; Fan, S. D-galactose protects the intestine from ionizing radiation-induced injury by altering the gut microbiome. *J. Radiat Res.* 2022, 63, 805−816.

(76) Homolak, J.; Babic Perhoc, A.; Virag, D.; Knezovic, A.; Osmanovic Barilar, J.; Salkovic-Petrisic, M. D-galactose might protect against ionizing radiation by stimulating oxidative metabolism and modulating redox homeostasis. *J. Radiat Res.* 2023, 64, 743−745.

(77) Yanar, K.; Simsek, B.; Atukeren, P.; Aydin, S.; Cakatay, U. Is D-Galactose a Useful Agent for Accelerated Aging Model of Gastrocnemius and Soleus Muscle of Sprague-Dawley Rats? *Rejuvenation Res.* 2019, 22, 521−528.

(78) Aksu, U.; Yanar, K.; Terzioglu, D.; Erkol, T.; Ece, E.; Aydin, S.; Uslu, E.; Çakatay, U. Effect of tempol on redox homeostasis and stress tolerance in mimetically aged Drosophila. *Arch Insect Biochem Physiol.* 2014, 87, 13−25.

(79) Shwe, T.; Pratchayasakul, W.; Chattipakorn, N.; Chattipakorn, S. C. Role of D-galactose-induced brain aging and its potential used for therapeutic interventions. *Experimental Gerontology.* 2018, 101, 13−36.

(80) Azman, K. F.; Zakaria, R. D-Galactose-induced accelerated aging model: an overview. *Biogerontology.* 2019, 20, 763−782.

(81) Homolak, J.; Kodvanj, I.; Toljan, K.; Babić Perhoč, A.; Virag, D.; Osmanovic, J.; Mlinarić, Z.; Smailovic, U.; Trkulja, V.; Hackenberger, B.; Lackovic, Z.; Salkovic-Petrisic, M. Separating science from science fiction: A non-existent enzyme is a primary driver of pathophysiological processes in galactose-induced rodent models of aging. *RG preprint* 2020, DOI: 10.13140/RG.2.2.31233.89449/1.

(82) Homolak, J.; Babic Perhoc, A.; Virag, D.; Knezovic, A.; Osmanovic Barilar, J.; Salkovic-Petrisic, M. D-galactose might mediate some of the skeletal muscle hypertrophy-promoting effects of milk-A nutrient to consider for sarcopenia? *Bioessays.* 2023, No. e2300061.

(83) Colucci, M.; Cervio, M.; Faniglione, M.; De Angelis, S.; Pajoro, M.; Levandis, G.; Tassorelli, C.; Blandini, F.; Feletti, F.; De Giorgio, R.; Dellabianca, A.; Tonini, S.; Tonini, M. Intestinal dysmotility and enteric neurochemical changes in a Parkinson's disease rat model. *Auton Neurosci.* 2012, 169, 77−86.

(84) Cui, H.; Elford, J. D.; Alitalo, O.; Perez-Pardo, P.; Tampio, J.; Huttunen, K. M.; Kraneveld, A.; Forsberg, M. M.; Myöhänen, T. T.; Jalkanen, A. J. Nigrostriatal 6-hydroxydopamine lesions increase alpha-synuclein levels and permeability in rat colon. *Neurobiol Aging.* 2023, 129, 62−71.

(85) Zhu, H. C.; Zhao, J.; Luo, C. Y.; Li, Q. Q. Gastrointestinal dysfunction in a Parkinson's disease rat model and the changes of dopaminergic, nitric oxidergic, and cholinergic neurotransmitters in myenteric plexus. *J. Mol. Neurosci.* 2012, 47, 15−25.

(86) Zarkovic, N. 4-hydroxynonenal as a bioactive marker of pathophysiological processes. *Mol. Aspects Med.* 2003, 24, 281−291.

(87) Milkovic, L.; Zarkovic, N.; Marusic, Z.; Zarkovic, K.; Jaganjac, M. The 4-Hydroxynonenal-Protein Adducts and Their Biological Relevance: Are Some Proteins Preferred Targets? *Antioxidants (Basel).* 2023, 12, 856.

(88) Zarkovic, N.; Butterfield, D. A. Neurodegeneration and regeneration: Antioxidants and redox signaling. *Free Radic Biol. Med.* 2022, 189, 154−156.

(89) Jaganjac, M.; Milkovic, L.; Zarkovic, N.; Zarkovic, K. Oxidative stress and regeneration. *Free Radic Biol. Med.* 2022, 181, 154−165.

(90) Dong, Y.; Hou, Q.; Lei, J.; Wolf, P. G.; Ayansola, H.; Zhang, B. Quercetin Alleviates Intestinal Oxidative Damage Induced by H2O2 via Modulation of GSH. *In Vitro Screening and In Vivo Evaluation in a Colitis Model of Mice, ACS Omega.* 2020, 5, 8334−8346.

(91) Wu, J.; Sun, B.; Luo, X.; Zhao, M.; Zheng, F.; Sun, J.; Li, H.; Sun, X.; Huang, M. Cytoprotective effects of a tripeptide from Chinese Baijiu against AAPH-induced oxidative stress in HepG2 cells via Nrf2 signaling. *RSC Adv.* 2018, 8, 10898−10906.

(92) Sies, H. Hydrogen peroxide as a central redox signaling molecule in physiological oxidative stress: Oxidative eustress. *Redox Biol.* 2017, 11, 613−619.

(93) Neill, S.; Desikan, R.; Hancock, J. Hydrogen peroxide signalling. *Curr. Opin Plant Biol.* 2002, 5, 388−395.

(94) Veal, E. A.; Day, A. M.; Morgan, B. A. Hydrogen peroxide sensing and signaling. *Mol. Cell* 2007, 26, 1−14.

(95) Ayala, A.; Muñoz, M. F.; Argüelles, S. Lipid Peroxidation: Production, Metabolism, and Signaling Mechanisms of Malondialdehyde and 4-Hydroxy-2-Nonenal. *Oxid. Med. Cell Longev.* 2014, 2014, No. 360438.

(96) Khoubnasabjafari, M.; Soleymani, J.; Jouyban, A. Avoid using spectrophotometric determination of malondialdehyde as a biomarker of oxidative stress. *Biomark Med.* 2018, 12, 551−554.

(97) Tsikas, D. Assessment of lipid peroxidation by measuring malondialdehyde (MDA) and relatives in biological samples: Analytical and biological challenges. *Anal. Biochem.* 2017, 524, 13−30.

(98) De Leon, J. A. D.; Borges, C. R. Evaluation of Oxidative Stress in Biological Samples Using the Thiobarbituric Acid Reactive Substances Assay *J. Vis Exp.* 2020, (159), DOI: 10.3791/61122-v.

(99) Perkovic, M. N.; Jaganjac, M.; Milkovic, L.; Horvat, T.; Rojo, D.; Zarkovic, K.; Ćorić, M.; Hudolin, T.; Waeg, G.; Orehovec, B.; Zarkovic, N. Relationship between 4-Hydroxynonenal (4-HNE) as Systemic Biomarker of Lipid Peroxidation and Metabolomic Profiling of Patients with Prostate Cancer. *Biomolecules.* 2023, 13, 145.

(100) Milkovic, L.; Cipak Gasparovic, A.; Zarkovic, N. Overview on major lipid peroxidation bioactive factor 4-hydroxynonenal as pluripotent growth-regulating factor. *Free Radic Res.* 2015, 49, 850−860.

(101) Lacković, Z.; Salković, M. Streptozotocin and alloxan produce alterations in rat brain monoamines independently of pancreatic beta cells destruction. *Life Sci.* 1990, 46, 49−54.

(102) Noble, E. P.; Wurtman, R. J.; Axelrod, J. A simple and rapid method for injecting H3-norepinephrine into the lateral ventricle of the rat brain. *Life Sci.* 1967, 6, 281−291.

(103) Erdoğan, M. E.; Aydın, S.; Yanar, K.; Mengi, M.; Kansu, A. D.; Cebe, T.; Belce, A.; Çelikten, M.; Çakatay, U. The effects of lipoic acid on redox status in brain regions and systemic circulation in streptozotocin-induced sporadic Alzheimer's disease model. *Metab Brain Dis.* 2017, 32, 1017−1031.

(104) Ilyasov, I. R.; Beloborodov, V. L.; Selivanova, I. A.; Terekhov, R. P. ABTS/PP Decolorization Assay of Antioxidant Capacity Reaction Pathways. *Int. J. Mol. Sci.* 2020, 21, 1131.

(105) Hrabárová, E.; Valachová, K.; Rapta, P.; Soltés, L. An alternative standard for Trolox-equivalent antioxidant-capacity estimation based on thiol antioxidants. Comparative 2,2'-azinobis[3-ethylbenzothiazoline-6-sulfonic acid] decolorization and rotational viscometry study regarding hyaluronan degradation. *Chem. Biodivers.* **2010**, *7*, 2191−2200.

(106) Marklund, S.; Marklund, G. Involvement of the superoxide anion radical in the autoxidation of pyrogallol and a convenient assay for superoxide dismutase. *Eur. J. Biochem.* **1974**, *47*, 469−474.

(107) Li, X. Improved pyrogallol autoxidation method: a reliable and cheap superoxide-scavenging assay suitable for all antioxidants. *J. Agric. Food Chem.* **2012**, *60*, 6418−6424.

(108) Homolak, J. In vitro analysis of catalase and superoxide dismutase mimetic properties of blue tattoo ink. *Free Radic Res.* **2022**, *56*, 343−357.

(109) Hadwan, M. H. Simple spectrophotometric assay for measuring catalase activity in biological tissues. *BMC Biochem.* **2018**, *19*, 7.

(110) Homolak, J. The effect of a color tattoo on the local skin redox regulatory network: an N-of-1 study. *Free Radic Res.* **2021**, *55*, 221−229.

(111) Ma, X.; Deng, D.; Chen, W.; Senturk, M.; Ma, X.; Deng, D.; Chen, W.; Senturk, M.*Inhibitors and Activators of SOD, GSH-Px, and CAT*; IntechOpen, 2017

(112) Percie du Sert, N.; Ahluwalia, A.; Alam, S.; Avey, M. T.; Baker, M.; Browne, W. J.; Clark, A.; Cuthill, I. C.; Dirnagl, U.; Emerson, M.; Garner, P.; Holgate, S. T.; Howells, D. W.; Hurst, V.; Karp, N. A.; Lazic, S. E.; Lidster, K.; MacCallum, C. J.; Macleod, M.; Pearl, E. J.; Petersen, O. H.; Rawle, F.; Reynolds, P.; Rooney, K.; Sena, E. S.; Silberberg, S. D.; Steckler, T.; Würbel, H. Reporting animal research: Explanation and elaboration for the ARRIVE guidelines 2.0. *PLoS Biol.* **2020**, *18*, No. e3000411.

(113) Rosseel, Y. lavaan: An R Package for Structural Equation Modeling. *Journal of Statistical Software.* **2012**, *48*, 1−36.